Stony Brook University

Effects of Lentiviral STAT3 and STAT3 Mutants on Cellular Proliferation and Tumor Formation

A Thesis Presented

by

Alkiviadis Stavros Pierrakeas

to

The Graduate School

in Partial Fulfillment of the

Requirements

for the Degree of

Master of Science

in

Biochemistry and Cell Biology

Stony Brook University

December 2016

Stony Brook University

The Graduate School

Alkiviadis Stavros Pierrakeas

We, the thesis committee for the above candidate for the

Master of Science degree, hereby recommend

acceptance of this thesis.

_____

Nancy C. Reich Marshall, Ph.D – Thesis Advisor
Professor - Department of Molecular Genetics and Microbiology

_____

Laurie T. Krug, Ph.D – Second Reader
Associate Professor – Department of Molecular Genetics and Microbiology

This thesis is accepted by the Graduate School

_____

Charles Taber
Dean of the Graduate School

Abstract of the Thesis

Effects of Lentiviral STAT3 and STAT3 Mutants on Cellular Proliferation and Tumor Formation

by

Alkiviadis Stavros Pierrakeas

Master of Science

in

Biochemistry and Cell Biology

Stony Brook University

2016

The mammalian Signal Transducers and Activators of Transcription (STAT) family of proteins includes seven STAT transcription factors that function in cytokine signaling pathways to activate gene expression affecting cell proliferation, cell growth, cell survival, and apoptosis. Cytokines such as interleukin-6 (IL-6), and several growth factors are able to bind to cell surface receptors, activate tyrosine kinase activity and promote downstream phosphorylation of STAT proteins. Cytokines associated with Janus kinases (JAKs) classically activate what has been termed JAK/STAT signaling pathways. Tyrosine-phosphorylated STATs are able to dimerize, enter the nucleus, and function by binding DNA and regulating gene transcription. One of the most well studied STAT proteins is STAT3, a necessary transcription factor for embryonic development and a critical component in various signaling mechanisms. STAT3 structurally and functionally resembles other members of the STAT family. Its activation requires phosphorylation of a specific tyrosine residue (Y705), and its activity can be enhanced even further by an additional serine residue phosphorylation (S727). Previous studies have shown that constitutively active STAT3 is present in many different cancers ranging from solid tumors (in the pancreas, prostate, mammary glands, lungs, etc.) to hematological cancers (including lymphomas and leukemia). Constitutive activation of STAT3 is believed to stimulate cell

proliferation, differentiation, and transformation of cells, while also repressing apoptosis, and thus, promote tumorigenesis. Defects in several stages of the JAK/STAT3 signaling pathway, including inactivating mutations in negative feedback regulators and hyperactivating mutations in upstream tyrosine kinases (JAKs), can produce constitutively active STAT3 proteins. STAT3 has also been found to function as a tumor suppressor in some cases, with inactivation of STAT3 resulting in more prominent tumor phenotypes (lung tissue).

The objective of my studies was to understand how STAT3 functions in different cells to either promote or inhibit tumorigenesis. The approach was to generate lentiviruses expressing STAT3, express lentiviral STAT3 in pre-malignant cells, and evaluate the proliferation and xenograph tumor formation of the cells. I created lentiviruses expressing wild-type (WT) STAT3 or one of several mutant STAT3 genes. We then ectopically expressed WT STAT3 or mutant STAT3 in pre-malignant pancreatic cells and pre-malignant lung cells. The cells were harvested from a mouse with p53 -/-; Lox-Stop-Lox K-RasG12D, and retroviral Cre was used to activate the K-Ras oncogenic mutation. The cells overexpressing WT STAT3 or mutant STAT3 were evaluated for cell behavior and proliferation, tumor growth, and tumor morphology. Both loss-of-function and gain-of-function STAT3 mutations were used to evaluate possible tumor-promoting or tumor-suppressing effects utilizing *in vitro* and *in vivo* analyses.

Results from our experiments depended on the tissue type, but in each case, STAT3 overexpression did not affect growth in tissue culture. However, when xenograph tumors were evaluated, STAT3 was found to promote differentiation. Pancreatic cells overexpressing WT STAT3 generated tumors more rapidly, but unexpectedly, histological evaluation showed extensive differentiation with more abundant glandular structures present after hematoxylin & eosin (H&E) and immunohistochemical (IHC) staining. Pancreatic cells expressing mutant STAT3 had similar growth rates as control cells, but they were also more differentiated. The lung cells were notably different. Lentiviral WT STAT3 reduced the rate of tumor growth, as did the STAT3 gain-of-function mutation. Cells with loss-of-function mutant STAT3 had similar growth rates as control. Regardless of the growth rate of lung cell tumors, they were also more differentiated, exhibiting a robust squamous cell carcinoma phenotype after staining tumor sections with H&E and antibodies for IHC. Additional studies are required in order to verify these conclusions, with several other cell lines yet to be examined and other mutant STAT3 constructs still requiring testing. Understanding how activation levels and concentration of

STAT3 affect cellular properties and tumor morphology will provide information on how to prevent STAT3's function in tumorigenesis, perhaps garnering a path for which drugs can be designed to limit STAT3 activity and/or decrease STAT3 concentration in tumor cells.

Table of Contents

List of Figures

List of Tables

List of Abbreviations

ADC	Adenocarcinoma
Brk	Breast Tumor Kinase
BSA	Bovine Serum Albumin
CML	Chronic Myeloid Leukemia
CTNNB1	*Beta*-Catenin
DMEM	Dulbecco's Modified Eagle Medium
DNA	Deoxyribonuecleic Acid
ECL	Enhanced Chemiluminescence
EGFP	Enhanced Green Fluorescent Protein
EGFR	Epidermal Growth Factor Receptor
FACS	Fluorescence-Activated Cell Sorting
FBS	Fetal Bovine Serum
FITC	Fluorescein Isothiocyanate
GAS	Gamma Interferon Activated Site
GFP	Green Fluorescent Protein
HEK	Human Embryonic Kidney
H&E	Hematoxylin and Eosin
IHC	Immunohistochemistry
IκB	Inhibitor of NF-κB (or κB)
IL	Interleukin
IRES	Internal Ribosome Entry Site
JAK	Janus Kinase

KRAS	V-Ki-Ras2 Kirsten Rat Sarcoma Viral Oncogene Homolog
KRT	Keratin
LB	Luria Broth
MAPK	Mitogen-Activated Protein Kinase
MEF	Mouse Embryonic Fibroblasts
NF-κB	Nuclear Factor Kappa-Light-Chain-Enhancer of Activated B Cells
mTOR	Mechanistic Target of Rapamycin
NSCLC	Non-Small Cell Lung Carcinoma
PDGFR	Platelet-Derived Growth Factor Receptor
PCR	Polymerase Chain Reaction
PI3K	Phosphotidylinositol-4,5-Bisphosphate 3 Kinase
PKC	Protein Kinase C
PTP	Protein Tyrosine Phosphatases
RIPA	Radioimmunoprecipitation Assay (Buffer)
SCC	Squamous Cell Carcinoma
SDS-PAGE	Sodium Dodecylsulfate Polyacrylamide Gel Electrophoresis
SH2	Src Homology 2 (Domain)
SOCS	Suppressor of Cytokine Signaling
Src	Proto-Oncogene Tyrosine-Protein Kinase Src (c-Src and v-Src)
STAT	Signal Transducer and Activator of Transcription
TAD	Transactivation Domain
TAE	Tris/Acetic Acid/EDTA Buffer
TBST	Tris Buffered Saline with Tween® 20

TE	Tris/EDTA Buffer
UV	Ultraviolet
VEGFR	Vascular Endothelial Growth Factor Receptor
WT	Wild-Type

Acknowledgements

I would like to thank Dr. Nancy Reich, Dr. Alexei Petrenko, Dr. Stephen D'Amico, and Dr. Marcin Stawowcyzk for all of the help and support throughout my time in Dr. Reich's lab. Dr. Reich was incredibly supportive, knowledgeable, and gracious for providing me with an opportunity to work in her lab throughout my Master's program. As the principle investigator and director of the project, she made sure I was up-to-date with all of the information involved in our current work by constantly challenging me to read and learn more. Our weekly meetings were a great opportunity to share ideas, engage with the rest of the group, and listen to what others had currently been working on.

I also want to specifically thank Dr. Alexei Petrenko for guiding me throughout my time in the lab. Many of the techniques, skills, and protocols I learned, as well as the theory and concepts for each experiment, were taught to me by him. I look forward to taking what I have learned from him, and from the rest of my peers in Dr. Reich's lab, and utilizing it to the best of my abilities in all of my future scientific endeavors.

This experience has been an excellent foundation for my scientific career. I am anxious to continue learning and building on the knowledge I have obtained to improve myself as an individual and as an aspiring scientist.

Chapter 1

Introduction

STAT3 is part of a group of transcription factors known as Signal Transducers and Activators of Transcription (STATs) (Shuai, *et al* 1992). The mammalian STAT family is comprised of seven STAT genes and proteins, each with similar structures and functional domains including an N-terminal domain, a coiled-coil domain, a DNA-binding domain, a Src homology-2 (SH2) domain, and a C-terminal transactivation domain (TAD) as pictured in Figure 1 (Reich and Liu, 2006). STAT transcription factors are essential proteins that regulate expression of genes involved in various cellular processes including cell cycle progression, development, tumor suppression, cell proliferation, apoptosis, and cellular transformation (Bromberg and Darnell Jr., 2000).

STAT proteins function in signal transduction by transmitting signals received from the cell surface to the nucleus of the cell, where they are able to promote gene transcription and activation (Darnell Jr., Kerr, and Stark, 1994). At the cell surface, ligands such as interferons or other cytokines, and growth factors, bind to cell surface receptors and initiate changes in downstream cellular signaling (Friedman, *et al* 1984; Larner, *et al* 1984). Cytokine and growth factor signaling can activate tyrosine kinases such as Janus kinases (JAKs) and result in tyrosine phosphorylation of STAT transcription factors (Velazquez, *et al* 1992; Argetsinger, *et al* 1993; Müller, *et al* 1993). Tyrosine phosphorylation of STATs promotes their dimerization and allows the STAT dimers to bind to regulatory sequences often found in the promoter regions of genes (Wegenka, *et al* 1994). The STAT proteins homodimerize or heterodimerize with one another by reciprocal interaction of their SH2 domains and phosphotyrosines (Figure 2) (Shuai, *et al* 1994).

Tyrosine phosphorylation regulates the nuclear translocation of the STAT1 founding member of the STAT family. However, most of the other STATs, including STAT3, do not require tyrosine phosphorylation and dimerization in order to translocate into and out of the nucleus (Liu, McBride, and Reich, 2005; Reich and Liu, 2006). STAT3 monomers are continuously imported into and exported out of the nucleus in an unphosphorylated state, however tyrosine phosphorylation remains essential for classical dimer formation and the ability

to bind a consensus DNA target, called a gamma interferon activated site (GAS), and stimulate gene expression (Wegenka, *et al* 1994).

STAT proteins respond to extracellular and intracellular tyrosine kinases by shifting between active and inactive states to allow for accurate gene expression and cell survival. STAT3 regulation is critical for normal cell differentiation and development, and a murine genetic knockout is embryonic lethal (Takeda, *et al* 1997). Interleukin-6 (IL-6) is a classical cytokine activator of STAT3 (Zhong, Wen, and Darnell Jr., 1994). IL-6 binding to the IL-6 receptor-gp130 complexes allows for phosphorylation and activation of associated JAK kinases and phosphorylation of STAT3 (Zhong, Wen, and Darnell Jr., 1994). In addition, other tyrosine kinases such as Src, Abl, epidermal growth factor receptors (EGFRs), platelet-derived growth factor receptors (PDGFRs), and vascular endothelial growth factor receptors (VEGFRs) can be responsible for phosphorylation and activation of STAT proteins (specifically STAT3) (Yu, *et al* 1995; Ilaria and Van Etten, 1996; Leaman, *et al* 1996; Garcia, *et al* 1997; Turkson, *et al* 1998). The critical tyrosine that is phosphorylated to activate the formation of STAT3 dimers is tyrosine 705 (Y705) (Shuai, *et al* 1994). Additionally, STAT3 serine 727 (S727) can be phosphorylated by specific serine kinases (PKC, mTOR, MAPK, etc.) increasingly activated in response to other cytokines and growth factor receptors (Wen, Zhong, and Darnell Jr., 1995; Decker and Kovarik, 2000). For proper regulation of JAK/STAT signaling, dephosphorylation mechanisms are essential to inactivate kinase and STAT activity and cause dissociation of STAT dimers into individual monomers. Protein Tyrosine Phosphatases (PTPs) such as CD45 and SHP1/SHP2 are involved in dephosphorylation of receptors, JAK kinases, and STAT3 dimers, deactivating the JAK/STAT signaling pathway (Irie-Sasaki, *et al* 2001; Han, *et al* 2006; Bard-Chapeau, *et al* 2011). Other negative regulators of JAK/STAT signaling are members of a protein family known as Suppressor of Cytokine Signaling (SOCS) (Starr, *et al* 1997). SOCS genes are induced by cytokine signaling and STAT transcription factors, and function to inhibit phosphorylated upstream kinases and receptors (i.e. JAK kinases and IL-6-induced receptors) (Starr, *et al* 1997). SOCS proteins have SH2 domains that bind to phosphotyrosine residues on JAKs and cytoplasmic domains of receptors, preventing downstream phosphorylation and signaling (Yasukawa, *et al* 1999; De Souza, *et al* 2002). The SOCS proteins also have a unique SOCS box domain that can recruit E3 ubiquitin ligases; in all, SOCS binding to JAKs and receptors can block enzyme activity, prevent STAT binding and phosphorylation, and target the

JAKs and receptors for ubiquitin-mediated proteosomal degradation (Yasukawa, *et al* 1999; Zhang, *et al* 1999; De Souza, *et al* 2002). The PTPs and the SOCS proteins both function as negative regulators of JAK/STAT signaling.

Defects in any of these activating or inactivating systems can lead to aberrant JAK/STAT signaling. JAK/STAT pathway defects have been shown to be major contributors to many human inflammatory diseases and cancers. STAT3 is one of the predominant members of the STAT family that is affected by dysregulation in the JAK/STAT pathway (Garcia and Rove, 1998). Research first showed that an artificially activated STAT3 could function as an oncogene (Bromberg, *et al* 1999). Mutations in the polypeptide sequence of STAT3 resulting in insertion of two cysteine residues within the SH2 domain created a constitutively dimerized and active STAT3 (STAT3 CC mutant) able to bind to DNA and promote transcription and gene expression resulting in transformation of cells (Bromberg, *et al* 1999). In many cases, constitutive activation of STAT3 is linked to tumorigenic phenotypes and characteristics of cancer cells, and this constitutive STAT3 activation is typically caused by oncogenic defects/mutations in upstream tyrosine kinases (Frame, 2002; Gao, *et al* 2007). Gain-of-function mutations in protein tyrosine kinases often result in increased phosphorylation and activation of STAT proteins, including STAT3 (Frame, 2002; Gao, *et al* 2007; Oku, *et al* 2010). Mutant Src tyrosine kinases have been shown to hyperactivate STAT signaling and cause oncogenesis (Yu, *et al* 1995). Hyperactivation of JAK tyrosine kinases have also been shown to result in overexpression of phosphorylated and activated STAT3 proteins (Bromberg, 2002; Levine, *et al* 2007). Similarly, serine kinases such as MAPK and cyclin-dependent kinase can be mutated in ways that result in amplified phosphorylation of serine residues on STAT3 proteins, making dimers more efficient at binding DNA and promoting transcription of downstream genes (Decker and Kovarik, 2000). Hyperactivation of STAT proteins can create a positive feedback loop as well. Activated STAT3, for example, promotes transcription and expression of genes encoding IL-6 and IL-10, and both IL-6 and IL-10 cytokines are involved in autocrine and paracrine signaling mechanisms that result in enhanced activation of the JAK/STAT3 signaling pathway (Zhong, Wen, and Darnell Jr., 1994). Activated STAT3 is able to interact with NF-κB as well, causing NF-κB to become constitutively activated and sequestered in the nuclei of cells; this promotes cell proliferation and cell survival as a result of STAT3/NF-κB co-regulation of genes involved in inflammation and oncogenesis (Yang, *et al* 2007).

Another major cause of hyperactive JAK/STAT signaling is defective negative feedback mechanisms within cells that prevent regulation and inactivation of this signaling pathway. As discussed earlier, specific tyrosine phosphatases and proteins such as SOCS are responsible for inhibiting JAK/STAT pathways. Research has shown that disruptions in SOCS1 and SOCS3 can stimulate STAT3 activation that leads to increased cell survival, cell proliferation, and cell growth, which is frequently implicated in cancers (Yoshikawa, *et al* 2001; He, *et al* 2003). Loss of function in tyrosine phosphatases including SHP1, SHP2, and CD45 reduces dephosphorylation of JAK kinases and STAT3, resulting in higher levels of phospho-STAT3/phospho-JAK that enhance STAT3 signaling (Irie-Sasaki, *et al* 2001; Han, *et al* 2006; Bard-Chapeau, *et al* 2011). Dual-specific phosphatases that are able to dephosphorylate STAT3 on particular serine and tyrosine residues can also be deactivated via mutations, preventing them from dephosphorylating and inactivating STAT3 (Liang, *et al* 1999).

Many mutations in the STAT3 protein itself have also been studied to observe how certain amino acid substitutions can affect JAK/STAT3 signaling processes, as well as to verify the importance of STAT3 in various signaling pathways. These studies have indicated essential amino acid residues that are responsible for activation and propagation of signaling mediated by STAT3. A tyrosine to phenylalanine mutation at position 705 (Y705F) has been reported to act as a dominant-negative mutation that inhibits phosphorylation, dimerization, and activation of STAT3 when expressed in cells, indicating that the tyrosine-705 residue is essential in IL-6 pathway signal transduction involving STAT3 (Kaptein, Paillard, and Saunders, 1996; Bromberg, *et al* 1998). Relatedly, mutations in S727 (i.e. S727A) can inhibit secondary phosphorylation of STAT3 and block maximal STAT3 activation, or mimic phosphorylation by substituting a permanent negatively charged amino acid for serine (S727E) (Qin, *et al* 2008). Mentioned earlier, two cysteine amino acid substitutions in the SH2 domain of STAT3 have been shown to produce constitutively dimerized and hyperactivated STAT3 proteins (Bromberg, *et al* 1999). Other works have determined additional gain-of-function mutants produced by single amino acid mutations at tyrosine 640 (Y640F) and lysine 658 (K658Y) of the SH2 domain in STAT3 (Pilati, *et al* 2012). Experiments involving the DNA-binding domain of STAT3 have shown that mutations targeting three valine residues to alanine (V461, V462, V463/VVV) or two glutamic acid residues to alanines (E434A, E435A/EE) results in STAT3 DNA-binding mutants that are able to interact and dimerize with other STAT monomers but have lost the ability to

associate with DNA and enhance gene expression (Horvath, Wen, and Darnell Jr., 1995). These DNA-binding mutants prevent transformation of cells and have a negative impact on oncogenesis stimulated by v-Src (Horvath, Wen, and Darnell Jr., 1995; Bromberg, *et al* 1998).

Mutations in any of these JAK/STAT3 signaling pathway components can affect cellular behavior and tissue phenotype, and have been clinically proven to be main contributors to the development of a number of cancers and other human ailments. Lung cancer, prostate cancer, mammary/breast cancer, and pancreatic cancer, among many others, have been known to arise due to defects in JAK/STAT3 signaling. Lung cancer continues to account for the most cancer deaths worldwide, and hyperactivity of JAK kinases, IL-6 signaling, and (rarely) constitutive activation mutations of STAT3 appear to contribute heavily to non-small cell lung carcinoma (NSCLC) development (Song, *et al* 2003). STAT3 signaling has been found to be constitutively active in most human pancreatic ductal adenocarcinomas and this constitutive activation appears to function together with oncogenic K-Ras (mutations) to promote progression of pancreatic tumorigenesis into more severe and differentiated histological phenotypes (Corcoran, *et al* 2011). Many aggressive mammary cancers exhibit high levels of IL-6 signaling as well as a loss of SOCS3 (negative feedback loop) function, which correlates with increased Brk (Breast Tumor Kinase) activity and elevated levels of phosphorylated and activated STAT3 (and STAT5b) commonly associated with oncogenesis (Gao, Cimica, and Reich, 2012). Finally, constitutively active STAT3 signaling has been associated with transformation of various cell types into tumorigenic cells, with one such example being in myeloid and hematopoietic cells in which STAT3 activity is vital for transformation caused by hyperactivation of Bcr-Abl signaling ultimately resulting in the advancement into chronic myeloid leukemia (CML) (Nair, Tolentino, and Hazlehurst, 2012). Counter-intuitively, STAT3 has been found to act as a tumor suppressor in lung cells containing oncogenic (hyperactive) K-Ras (K-RasG12D), reducing K-Ras-induced lung tumorigenesis (Grabner, *et al* 2015). Because STAT3 is a significant protein involved in many pathways that are often deregulated in cancers, it is important to study its function and proposed mechanism of action in detail to identify where treatments and inhibitors can be developed to neutralize its specific tumorigenic properties.

Our research focused on the function of individual STAT3 protein in regards to its role in tumorigenesis, tumor growth/development, and tumor morphology. We used lentiviruses containing STAT3 WT and several STAT3 mutants described earlier (STAT3 Y705F, STAT3

CC, STAT3 EE, and STAT3 VVV) to ectopically express STAT3 (WT or mutant) in various cell types. These mutations are known to affect STAT3 functioning in different ways. STAT3 Y705, STAT3 EE, and STAT3 VVV mutants inhibit STAT3 activation by preventing phosphorylation/dimerization or inhibiting binding of STAT3 homodimers and heterodimers to promoter regions of DNA/genes. STAT3 CC is presumably a constitutively activating mutation that enables STAT3 to remain dimerized, resulting in amplification of STAT3 signaling. Each of these five STAT3 constructs were integrated into the genome of cells by lentiviruses and expressed in cells that have endogenous STAT3. Lentiviral transductions were performed on several different cell types originating from different human tissues (mammary) and murine tissues (mouse embryonic fibroblasts, pancreas, lungs), either non-transformed or transformed by activated K-Ras (Ischenko, Petrenko, and Hayman, 2014; Ischenko, Liu, *et al* 2014).

The main cell lines used in our study originated from heterogeneous populations of murine pancreatic cells and lung cells; two clonal cell lines were derived from each population. The pancreas 2 and pancreas 16 clonal cell lines are PDX1+ pre-malignant pancreatic cells, obtained from Alexei Petrenko (Ischenko, Petrenko, and Hayman, 2014). They were originally generated from p53-/-; Lox-Stop-Lox-K-RasG12D mice, and the oncogenic K-RasG12D gene was activated by introducing retroviruses containing Cre-recombinase (Ischenko, Petrenko, and Hayman, 2014). Both of these pancreas cell clones are stem cell-like in nature and prone to give rise to tumorigenic cells that metastasize. Additionally, these clones/cells, and other pancreatic cells exhibiting stem cell-like phenotypes, are the cells most susceptible to K-Ras mutations and most commonly responsible for tumor development in the presence of oncogenic K-Ras (Friedlander, *et al* 2009). Specifically, these clones are predominantly SCA1- and differentiated to different extents based on the degree to which they activate and inactivate SCA1 and CD133 expression (Ischenko, Petrenko, and Hayman, 2014). The pancreas 16 clone cells are a less differentiated cell lineage than the pancreas 2 clone cells as the pancreas 16 cells (CD133-/SCA1-) do not express CD133 or SCA1 (Ischenko, Petrenko, and Hayman, 2014). Pancreas 2 clone cells have begun to express CD133 and SCA1, resulting in a more differentiated population that is CD133+/- and SCA1+/- (Ischenko, Petrenko, and Hayman, 2014).

The lung 8 and lung 28 clonal cell lines also came from a heterogeneous population of oncogenic K-RasG12D and p53-/- cells that can be individually identified based on specific levels of genes such as p63, KRT15, and SOX2 (Ishenko, Liu, *et al* 2014). Lung 8 clone cells

are p63+Sox2+KRT15- whereas Lung 28 clone cells are p63+Sox2-KRT15- (Ischenko, Liu, *et al* 2014). These clones are comprised of pre-malignant and untransformed cells, and like the two pancreas clones, they contain different degrees of expression of certain genes that make Lung 28 clone cells less differentiated than Lung 8 clone cells (Ischenko, Liu, *et al* 2014).

The STAT3 lentiviral plasmids administered in transductions encoded GFP and fluorescence was used to isolate cells by flow cytometry. Employing this method, we were able to observe how ectopic expression of each mutant STAT3 construct or STAT3 WT altered cellular properties such as proliferation or differentiation (*in vitro* and *in vivo*), transformation by focus-formation assay in tissue culture (*in vitro*), and tumor development with xenographs in nude mice (*in vivo*). Lentiviral STAT3 expressing cells were introduced subcutaneously in nude mice and tumor progression was monitored. Tumors were harvested from sacrificed animals and examined by histology and hematoxylin and eosin (H&E) stain to characterize the effects of STAT3 protein expression (WT and mutants), and better understand the role of STAT3 in cancer.

Chapter 2

Materials and Methods

Plasmid Preparation

DH5α (*E. coli*) competent cells were transformed with FoxJ1-IRESEGFP lentiviral vector provided by Ihor Lemischka (Mount Sinai Medical Center, NY) and pCDH CMV MSCV E2F1GFP lentiviral vector provided by Marcin Stawowcyzk (Stony Brook University, NY). Transformed D□□α□cells were plated and grown on LB/agar plates containing 100 ug/ul carbenicillin. Bacterial colonies were chosen and grown in cultures; bacterial cultures were used to perform midipreps using the Promega PureYield™ Plasmid Midiprep System in order to isolate the pCDH CMV MSCV E2F1GFP and FoxJ1-IRESEGFP vectors.

Sequencing and PCR amplification of STAT3 WT and STAT3 Mutant Plasmids

Five STAT3 plasmids that were sequenced and amplified were:

(1) HA-h-STAT3 Wild-Type
(2) pRC/CMV-STAT3 Y705F
(3) pRC/CMV-STAT3 CC
(4) TOPO-STAT3 EE
(5) TOPO-STAT3 VVV

Sequencing of each STAT3 plasmid was performed by the DNA Sequencing Facility at Stony Brook University. The sequencing primers were ordered from Eurofins Genomic. Sequencing data was analyzed using BLAST and CLC Sequence Viewer 7 to compare the five plasmids to a wild-type murine STAT3 sequence obtained from GenBank; the mutations of each mutant plasmid were verified in terms of presence and location within the STAT3 gene. The sequencing primers used for plasmid sequencing and verification are listed in Table 1.

Sequenced STAT3 plasmids (mutant and WT) were used as templates to amplify the STAT3 cDNA by polymerase chain reaction (PCR) for cloning into the lentiviral vectors. The PCR primers used for amplification of each STAT3 (WT or mutant) gene are listed in Table 2. PCR primers were obtained from Eurofins Genomic; colored sections in the oligonucleotide

sequence of the PCR primers (Table 2) represent cleavage/digestion sites for specific restriction endonuclease enzymes.

For the WT STAT3, STAT3 Y705F mutant, and STAT3 CC mutant, PCR amplification reactions were done using three different pairs of primers: (1) PCR2 + PCR3, (2) PCR2 + PCR4, and (3) PCR10 + PCR11. Two different pairs of primers were used in the PCR amplification reactions of the STAT3 EE and STAT3 VVV mutants: (1) PCR3 + PCR5 and (2) PCR10 + PCR11. In total, 13 products were accumulated after the PCR amplifications were completed. PCR products amplified with primers PCR10 and PCR11 were flanked with *SfiI* restriction enzyme cut sites containing the general cleavage site sequence GGCCNNNN^NGGCC. Plasmids amplified with PCR primers PCR3 and PCR4 contained GC^GGCC_GC cleavage sites for the *NotI* restriction endonuclease. Plasmids amplified with PCR2 and PCR5 primers were flanked by G^AATTC *EcoRI* cleavage sites. The PCR parameters were set to a 95°C initial denaturation for 5 minutes, followed by 35 cycles of: 95°C denaturation phase for 1 minute, 60°C annealing phase for 30 seconds, 72°C elongation phase for 3 minutes, and a final elongation phase at 72°C for 10 minutes.

Restriction Endonuclease Cleavage and Digestion of DNAs

PCR products were digested with a specific restriction endonuclease or set of endonucleases depending on the primers used for PCR amplification. cDNAs amplified with PCR2 + PCR3, PCR2 + PCR4, or PCR3 + PCR5 primer sets were digested with *NotI* and *EcoRI* enzymes; cDNAs amplified with PCR10 + PCR11 were digested with *SfiI* restriction enzyme. All digested products (~200 ng) were run on a 0.8% agarose gel with a 10 kb DNA ladder used as a reference for size of the DNA fragments. PCR amplification and digestion generated 13 products able to be used for lentiviral production:

1. (HA-h) STAT3 WT amplified with PCR2 + PCR3 and digested with *NotI*/*EcoRI*
2. (HA-h) STAT3 WT amplified with PCR2 + PCR4 and digested with *NotI*/*EcoRI*
3. (HA-h) STAT3 WT amplified with PCR10 + PCR11 and digested with *SfiI*
4. (pRC CMV) STAT3 Y705F amplified with PCR2 + PCR3 and digested with *NotI*/*EcoRI*
5. (pRC CMV) STAT3 Y705F amplified with PCR2 + PCR4 and digested with *NotI*/*EcoRI*
6. (pRC CMV) STAT3 Y705F amplified with PCR10 + PCR11 and digested with *SfiI*
7. (pRC CMV) STAT3 CC amplified with PCR2 + PCR3 and digested with *NotI*/*EcoRI*

8. (pRC CMV) STAT3 CC amplified with PCR2 + PCR4 and digested with *NotI*/*EcoRI*
9. (pRC CMV) STAT3 CC amplified with PCR10 + PCR11 and digested with *SfiI*
10. (TOPO) STAT3 EE amplified with PCR3 + PCR5 and digested with *NotI*/*EcoRI*
11. (TOPO) STAT3 EE amplified with PCR10 + PCR11 and digested with *SfiI*
12. (TOPO) STAT3 VVV amplified with PCR3 + PCR5 and digested with *NotI*/*EcoRI*
13. (TOPO) STAT3 VVV amplified with PCR10 + PCR11 and digested with *SfiI*

Following the PCR fragment digestions, *DpnI* restriction endonuclease digestion was conducted on all 13 samples to degrade all methylated (plasmid) DNA, leaving behind only the unmethylated (amplified) cDNA as the product.

The pCDH CMV MSCV E2F1GFP vector was cut with *NotI* and *EcoRI* and the FoxJ1-IRESEGFP vector was cut with *SfiI*. All vectors and STAT3 cDNAs were purified via phenol-chloroform extraction and isopropanol precipitation, and the final products were dissolved in TE (pH 8.0). In general, phenol-chloroform extraction/isopropanol washing was done after PCR amplification as well as after each series of enzymatic digestions.

Ligation of Vector(s) with STAT3 Constructs

Concentrations of the two vectors and the 13 STAT3 cDNA fragments were measured using the Thermo Scientific NanoDrop ND-2000 1-Position Spectrophotometer. A 2:1 construct to vector ratio, in terms of concentration (ug/ul), was required for each ligation reaction. After digestion of both vectors and the STAT3 cDNAs with *SfiI* or *NotI* and *EcoRI*, the ligation reactions were performed to incorporate the STAT3 (WT or mutant) insert into (one of) the lentiviral vector(s). After the ligations were complete, phenol-chloroform extraction or use of the WizardGel® SV Gel and PCR Clean-Up System was performed on each reaction.

Transformation of TAM1 Competent *E. coli* Cells with Ligation Products and PCR Screening of Cloned Bacterial Colonies

RapidTrans™ TAM1 competent *E. coli* cells (active motif) were transformed with each of the 13 STAT3 ligation products and plated on LB/agar plates containing 100 ug/ul carbenicillin. Both lentiviral vectors were also cloned into TAM1 Competent *E. coli* cells and plated similarly. Each of the 5 STAT3 lentiviral constructs was prepared separately. Eight

colonies from each plate of transformed bacteria were screened through PCR (same parameters as previously used). Gel electrophoresis was conducted on a 1.6% agarose gel to evaluate the presence of the recombinant DNA. Each of the 13 STAT3 constructs generated gave multiple recombinant (positive) bacterial colonies after transformation; therefore, midipreps were done on several positive bacterial colonies from each, producing a number of samples to be used for transfection of cells and lentiviral production. Subsequently, concentrations were taken using the NanoDrop ND-2000 1-Position Spectrophotometer. For each STAT3 lentiviral construct, digestions with either *SfiI* or *NotI*/*EcoRI* were done, depending on how the vector and insert were cut and ligated originally, and run on a 0.8% agarose gel to view whether or not an insert would drop out of the construct. This was used as another measure to verify the efficiency of ligation, recombination, and extraction. Additionally, glycerol stocks were made with every positive bacterial clone from each of the STAT3 lentiviral constructs and stored at -80°C.

Transfection of HeLa Cells with Lentiviral STAT3 Constructs

HeLa cells were grown in 6 cm tissue culture plates and maintained in 3 ml of DMEM (Dulbecco's Modified Eagle Medium) containing 10% FBS and streptomycin/penicillin. Prior to transfection, the medium of each plate was aspirated and replaced by fresh DMEM (+ FBS and pen/strep). Transfections required 6 ug of STAT3 lentiviral construct mixed with MIRUS Trans-IT transfection reagent and OPTI-MEM; all STAT3 lentiviral constructs were transfected into HeLa cells. At the time of transfection, it was important that the HeLa cells were 50-80% confluent. The following day, cells were observed under a UV-microscope to evaluate the lentiviral encoded GFP expression and fluorescence. Flow cytometry and FACS analysis was performed to provide a more accurate measurement as to how many cells were fluorescent after each of the transfections. Based on transfection efficiencies and fluorescence detected, samples of lentiviral constructs were categorized until the most effective samples yielding the greatest fluorescence and GFP expression were determined; at least one sample from each of the 5 major lentiviral STAT3 constructs (WT and four mutants) was maintained.

Transfected HeLa Cell Lysis and Western Blotting

Protein lysates were made from each of the transfected HeLa cell plates; these lysates were prepared in RIPA lysis buffer containing 25mM Tris-HCl (pH 7.6), 150 mM NaCl, 1% NP-40, 1% sodium deoxycholate, 0.1% sodium dodecyl sulfate (SDS), and general protease inhibitor. Lysates were used to evaluate STAT3 expression by Western blotting utilizing a 10% SDS-polyacrylamide gel. Protein concentrations of the lysates were measured by BioRad protein assay using the Spectronic Genesys 5 spectrophotometer. A protein assay standard curve was generated with bovine serum albumin (BSA) and concentrations for all protein lysates were determined based on their given absorbance values in reference to the curve. Western blots were run using 60-80 ug of each protein sample. Alongside each sample, a protein ladder was also run to give a size reference to the bands obtained from the Western blot, and to provide a marker for a successful membrane transfer. After electrophoresis (SDS-PAGE) was complete, membrane transfers were carried out for approximately 80 minutes using a nitrocellulose membrane(s). Following transfer, the membrane was washed with Tris Buffered Saline with Tween® 20 (TBST), stained with Ponceau S to confirm protein transfer, and blocked by submerging the membrane in blocking buffer containing TBST and milk (1 gram of powdered milk in 20 ml of TBST) for 40 minutes. Following this, 1 ul of purified mouse anti-STAT3 monoclonal antibody (primary antibody – BD Transduction Laboratories™) diluted in a separate TBST and milk solution (total volume of 2 ul) was added to the membrane. The membrane was enclosed in a plastic pouch containing the primary antibody/buffer solution and left to incubate overnight at 4°C while gently shaking. After a 24-hour incubation period, the primary antibody was removed, the membrane was sequentially washed with TBST, and a secondary (mouse monoclonal – ECL™ anti-mouse IgG, Horseradish Peroxidase linked whole antibody) antibody was administered to the membrane (7.5 ul secondary antibody diluted in 20 ml of buffer); the secondary antibody was left to contact the membrane for 30 minutes. Finally, another round of washing was done, followed by soaking the membrane in 2 ml Enhanced Chemiluminescence (ECL) solution for 5 minutes and detection by X-ray film. Western blot for MAPK (ERK1/2) protein expression was used as a loading control (BD Transduction Laboratories™ - mouse anti-MAPK monoclonal antibody).

Generation of Lentiviruses for Each of the STAT3 Constructs

Two lentiviral packaging plasmids, PsPax2 and pMD2.G, were transformed into DH5α□cells□□□psPax2 is a 2nd generation lentiviral packaging plasmid and pMD2.G is an envelope expressing plasmid containing a VSV-G tag (Addgene, Cambridge, MA, USA, Plasmids 12259 and 12260, 2006). The packaging plasmids were purified via phenol-chloroform extraction and isopropanol wash.

For lentiviral production, HEK-293T cells were cultured in 10 cm tissue culture plates containing DMEM and FBS with streptomycin/penicillin. HEK-293T cells were transfected with each packaging plasmid in addition to a specific STAT3 plasmid (construct) using the formula:

- 14 ug STAT3 plasmid (WT, Y705F, CC, EE, VVV)
- 4 ug PsPax2 packaging plasmid
- 2 ug pMD2.G enveloping plasmid
- 1 ml OPTI-MEM medium
- 40 ul Transfection reagent (MIRUS Trans-IT)

HEK-293T cells were left in DMEM + transfection solution for 12-15 hours before changing the medium to fresh (13 ml) DMEM and allowing the cells to continue to grow/divide. At this point, the 293T cells were viewed under a UV microscope to observe fluorescence. Harvesting of lentiviruses began 24 hours later and was performed every 12 hours for three cycles. Lentiviruses were collected along with the medium and passed through a syringe attached to a 0.45 micron filter. Lentiviral solutions for each STAT3 construct were stored as 3 ml aliquots at -80°C.

Lentiviral Infections

The main clonal cell lines studied in these experiments were two murine pancreatic cell lines (Clones 2 and 16) (Ischenko, Petrenko, and Hayman, 2014) and two murine lung cell lines (Clones 8 and 28) (Ischenko, Liu, *et al* 2014). These were pre-malignant cells isolated from mice with a p53-/- genotype and expressing the oncogenic mutant K-RasG12D gene. The cell clones were derived from heterogeneous populations of either lung or pancreas cells. Before lentiviral infection, each cell line was grown in 6 cm tissue culture plates until 50-70% confluent.

Once cells attached, DMEM medium was removed from the plates; in place, 3 ml of lentiviral solution (of a particular STAT3 construct or vector) was added to the dish, and this was done with all of the lentiviral constructs using all cell lines. Cells were incubated at 37°C and 5% CO_2 for 48 hours. Once two days had passed and all cells were approximately 100% confluent, the lentiviral medium was removed from each plate and the cells were split into three 10 cm plates: (1) cells from one plate were lysed and the protein lysates were used to produce Western blots, (2) cells from the second plate were suspended in Thermo Fisher Scientific Synth-A-Freeze Cryopreservative Medium and stored (frozen) to maintain infected cell stocks, and (3) the third plate of each of the infected cells was ultimately used to inject mice subcutaneously. Infected cells were also subjected to various *in vitro* assays including soft agar assays, focus-formation assays, and suspension (sphere-forming) assays (conducted by Alexei Petrenko). Soft agar assays monitored cell growth and colony formation on substrates comprised of 0.25% Noble agar/DMEM containing 10% FBS and antibiotic/antimycotic (Invitrogen). For suspension assays, cells were cultured on plates lacking adhesive properties while immersed in CnT-17 medium containing exogenous growth factors. This was performed to observe if cells were able to survive being detached and clustered together, and if they could be rejuvenated to grow after re-plating on adhesive tissue culture plates.

Evaluation of Tumor Formation in Nude Mice

All animal studies were approved by the Institutional Animal Care and Use Committee at Stony Brook University. Infected cells from each lentiviral infection were trypsinized, pelleted and collected via centrifugation (1,000 rpm for 3 minutes), and resuspended in OPTI-MEM solution. Approximately 100,000 (10^5) cells were placed into labeled microcentrifuge tubes in a volume of 100 ul OPTI-MEM. Nude mice (obtained from the Jackson lab) were injected subcutaneously with 10 ul of the infected cell solution (~10^4 cells) in four separate regions of the body: an injection above each of the two shoulders of the front legs and two injections in the lower abdominal region, above the shoulders of the rear legs. Mice were examined frequently until tumors began to develop; once tumors appeared, their growth was monitored every two days until tumors were of an appropriate size (approximately 4 um in diameter) or appeared to inhibit quality of life. Mice were euthanized through asphyxiation by carbon dioxide and each of the tumors was excised from the organism. Tumors produced from each lentiviral construct

were collected and sent to the Histology Core Lab in the Health Sciences Center at Stony Brook University for (paraffin) embedding, sectioning, and H&E staining. Other sections of each tumor were also prepared for immunohistochemistry (IHC) using specific antibodies for keratin 19, keratin 15, p63, and *beta*-catenin. Keratin 19 (KRT19) and p63 were used to stain for squamous cell carcinoma morphologies in lung tumor samples (Abbas, *et al* 2011), whereas *beta*-catenin (CTNNB1) and keratin 19 stained for ductal morphologies (adenocarcinoma) in pancreatic tumor samples (Dabeva, *et al* 1997; Zeng, *et al* 2006). Once H&E stained and IHC stained tumor sections were retrieved, tumor characteristics and phenotype (histology) were analyzed and compared to one another to determine if STAT3 or mutant STAT3 constructs influence tumor development, tumor differentiation, tumor growth and/or morphology. Tumor growth charts were also constructed to track the progression and rate of tumor growth/development produced from ectopic expression of each lentiviral STAT3 construct.

STAT3 Mutagenesis to Generate STAT3 S727E, STAT3 K658Y, and STAT3 Y640F – Site-Directed Mutagenesis

To generate three STAT3 genes with site-specific mutations, primers were designed to produce STAT3 S727E, STAT3 K658Y, and STAT3 Y640F. Each primer contained a mutated nucleotide or mutated dinucleotide sequence flanked by approximately 20 nucleotides. This mutated nucleotide sequence altered the codon to encode for a specific single amino acid change in each construct. The primers used for mutagenesis were:

STAT3 Y640F → Adenine mutated to a thymine at position 1919.

(1) Reverse (R): 5'-CTGCTGCTTGGTGAATGGCTCTACAGACTGGATC-3'

(2) Forward (F): 5'-GATCCAGTCTGTAGAGCCATTCACCAAGCAGCAG-3'

STAT3 S727E → Adenine mutated to a thymine at position 1972; guanine mutated to a thymine at position 1974.

(3) R: 5'-CAATGAATCTAAAGTGCGGGGTTCCATCGGCAGGTCAATGGTATT-3'

(4) F: 5'-AATACCATTGACCTGCCGATGGAACCCCGCACTTTAGATTCATTG-3'

STAT3 K658Y → Thymine mutated to a guanine at position 2179; cytosine mutated to an adenine at position 2180; cytosine mutated to adenine at position 2181.

(5) R: 5'-ATGTTGGTCGCATCCATGATATAATAGCCCATGATGATTTCAGC-3'

(6) F: 5'-GCTGAAATCATCATGGGCTATTATATCATGGATGCGACCAACAT-3'

PCR mutagenesis was performed using STAT3 WT as the template. Three separate reactions were made using a different set of forward and reverse primers in each reaction to create the desired mutants. All three reactions were mixed and placed into a PCR thermal cycler; PCR was run at 95°C initial denaturation for 5 minutes, followed by 20 cycles of: 30 second denaturation at 95°C, primer annealing for 30 seconds at 58° C, extension for 25 minutes at 72°C, and a final extension period of 25 minutes at 72°C to finish the process. Each sample was digested with *DpnI* restriction enzyme for 2 hours at 37°C. Subsequent transformation into TAM1 *E. coli* cells, growth of transformed bacteria in liquid cultures, midipreps on selected bacterial colonies, and purification of plasmids were performed as previously described. Following confirmation of the mutation by DNA sequence analysis, lentiviruses were produced for the newly created STAT3 mutants. These mutants were generated later on within the timeline of the study and have yet to be used in transductions of cells and injections into mice.

Sequencing Oligonucleotide Primers

Sequencing Primer Name	Oligonucleotide (Primer) Sequence (5'→3')
PR STAT3.1 Direct	5'-ATGGCTCAGTGGAACCAGCT-3'
PR STAT3.2 Reverse	5'-GAAACACCAACGTGGCATGT-3'
PR STAT3.3 Direct	5'-ACATGGATCTGACCTCGGAG-3'
PR STAT3.4 Reverse	5'-AAGTTAGGAGTTTCAGACGA-3'

Table 1: *Table indicating the names of the sequencing primers used for DNA sequencing of each STAT3 plasmid in addition to their oligonucleotide sequence (5'→3' direction).* Two forward (direct) primers and two reverse primers were used to sequence the entire 2,313 basepair (bp) sequence of each mutant or WT STAT3 gene.

PCR Oligonucleotide Primers

PCR Primer Name	Oligonucleotide (Primer) Sequence (5'→3')
PCR2	5'-CTCTTTCTTGCAG**GAATTC**CGCCGCGACCAGCCAGG-3'
PCR3	5'-CTTCTTTTAA**GCGGCCGC**TCACATGGGGGAGGTAGCACAC-3'
PCR4	5'-CTTCTTTTAA**GCGGCCGC**AAGTTAGGAGTTTCAGACGA-3'
PCR5	5'-CTCTTTCTTGCACTGCA**GAATTC**GCCCTTAGATC-3'
PCR10	5'-CTCTGAATTC**GGCCATTACGGCC**ATGGCTCAGTGGAACCAGCTGCA-3'
PCR11	5'-TCTTGAATTC**GGCCGAGGCGGCC**TCACATGGGGGAGGTAGCACACT-3'

Table 2: *PCR (Polymerase Chain Reaction) primers used for PCR amplification of each of the five STAT3 genes (four mutants and one WT).* PCR10 and PCR11 primers contained a *SfiI* restriction endonuclease cleavage site (GGCCNNNN^NGGCC - **Black**). PCR3 and PCR4 primers contained a *NotI* restriction endonuclease cleavage site (GC^GGCC_GC - **Red**). PCR2 and PCR5 primers contained an *EcoRI* restriction endonuclease cleavage site (G^AATTC - **Blue**).

Chapter 3

Results

Cloning WT and Mutant STAT3 Genes Into FoxJ1-IRESEGFP Lentiviral Vector

Several mutations in STAT3 have been documented to affect STAT3 function that either promote or repress tumorigenicity and cell proliferation in cells. We focused on four mutant STAT3 plasmids in addition to STAT3 WT in order to examine how their expression and/or overexpression affected cell growth, cell proliferation, and tumor growth/development. The mutants were chosen based on the changes in STAT3 functionality they represent; certain mutations lead to increased activity of STAT3 while others inhibit STAT3 activation and function (Figure 1). STAT3 Y705F contains a mutation in an essential tyrosine residue (a.a. 705) that has been shown to be the site of phosphorylation by Janus Kinases in the JAK/STAT signaling pathway (Kaptein, *et al* 1996). Conversion of tyrosine-705 to phenylalanine produces a dominant-negative mutation in the STAT3 protein (Kaptein, *et al* 1996; Bromberg, *et al* 1998). The STAT3 CC mutant contains two cysteine residues (positions 661 and 663) substituted in place of two alanine residues located in the C-terminal loop of the SH2 domain of STAT3 (Bromberg, *et al* 1999). This mutation produces extra covalent bond linkages (disulfide linkages) between STAT3 monomers that result in dimerization of STAT3; consequently, STAT3 CC is classified as a hyperactive mutation that maintains STAT3 dimers (Bromberg, *et al* 1999). STAT3 EE and STAT3 VVV mutants have been classified as DNA-binding mutants; in both cases, specific alanine residues in the DNA binding domain of STAT3 have been substituted in for either two glutamic acid residues (E434A, E435A) or three valine residues (V461A, V462A, V463A) to produce these two negative mutants (Bromberg, J., Horvath, C.M, *et al* 1998). Prior to PCR cloning, sequencing of each of the five STAT3 plasmids verified the identity of the STAT3 mutations (Figure 1). Sequencing results showed that the mutated STAT3 plasmids contained the appropriate nucleotide changes within the respective genes, as seen in Table 3. These alterations encoded for the desired single amino acid mutation for each of the mutant STAT3 proteins.

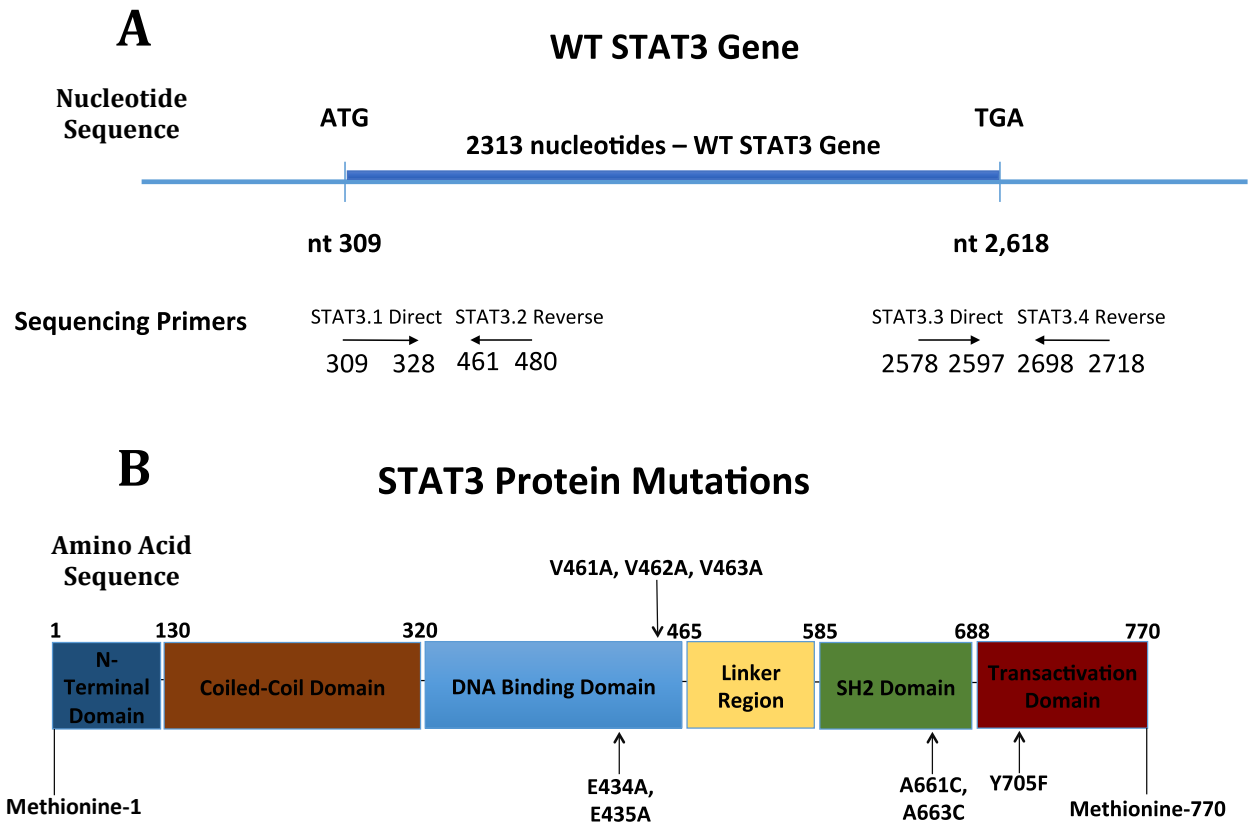

Figure 1: (A) *Sequencing primer hybridization sites on the STAT3 gene.* Diagram showing STAT3 (WT) gene in relation to the four constructed sequencing primers (STAT3.1 Direct, STAT3.2 Reverse, STAT3.3 Direct, and STAT3.4 Reverse). The primers were used to sequence STAT3 WT plasmid in addition to the four STAT3 mutants. Sequencing information was used to determine the presence and location of the mutated nucleotides within each mutant STAT3 plasmid prior to their use in future experiments. (B) *STAT3 protein diagram showing the domains that comprise a STAT3 monomer and the respective mutations of each of the STAT3 mutants.* The diagram shows the mutations in the amino acid sequence of all four STAT3 mutants, as verified through sequencing. STAT3 Y705F mutation is located in the transactivation domain (TAD), STAT3 CC is located within the SH2 domain, and the STAT3 EE and STAT3 VVV mutations are present in the DNA binding domain. Additional STAT3 mutants produced via site-directed mutagenesis (not tested yet) are located in the TAD (S727E) as well as the SH2 domain (Y640F and K658Y).

Plasmid	Change in Nucleotide Sequence	Change in Amino Acid Sequence	Mutation Type
STAT3 WT	No Mutation - WT	No Mutation - WT	No Mutation - WT
STAT3 Y705F	AAG to TAC at position 2,107 to 2,109	Tyr to Phe at position 705	Dominant Negative Mutation
STAT3 CC (A661C, N663C)	GCG to TGT at position 1,984 to 1,986; AA to TG at position 1,991 to 1,992	Ala to Cys at position 661; Asn to Cys at position 663	Constitutively Active Mutation
STAT3 EE (E434A, E435A)	C to A at position 1,298; C to A at position 1,301	Glu to Ala at position 434; Glu to Ala at position 435	DNA Binding Mutation
STAT3 VVV (V461A, V462A, V463A)	T to C at position 1,382; T to C at position 1,385; To to C at position 1,388	Val to Ala at position 461; Val to Ala at position 462; Val to Ala at position 463	DNA Binding Mutation

Table 3: *Nucleotide changes and their respective amino acid alterations for each of the STAT3 mutant plasmids with respect to wild-type STAT3 sequences.* STAT3 Y705F contains changes of the AAG nucleotide sequence to TAC resulting in a tyrosine to phenylalanine mutation at position 705 of the STAT3 protein. STAT3 CC contains two nucleotide sequence changes of GCG to TGT and AA to TG that produce two alanine to cysteine amino acid substitutions at positions 661 and 663 of the STAT3 protein. A single nucleotide change in two GAG codons results in two GCG codons that produce glutamic acid to alanine substitutions at positions 434 and 435 of the STAT3 EE mutant. Three valine residues are converted into alanine amino acid residues by single nucleotide substitutions of T to C in three consecutive codons of the STAT3 VVV mutant.

Lentiviral constructs were produced by cloning each STAT3 insert into a FoxJ1-IRESEGFP lentiviral expression vector or pCDH CMV MSCV E2F1EGFP lentiviral vector. Lentiviral vectors are well-established vehicles that allow for high-efficiency infection and expression of a gene of interest in both dividing and non-dividing mammalian cells (*SBI: Systems Bioscience* User Manual, 2012). Our research required infection of various cancer cell lines, many of which are known to have irregular growth patterns and altered proliferation rates, therefore lentiviral vectors were chosen as an optimal means for introducing the STAT3 genes. By cloning each STAT3 insert into a lentiviral vector, there was an increased chance of permanent STAT3 insertion into the genome of and stable exogenous STAT3 expression in

various cell types. We used FoxJ1-IRESEGFP vector, which is a 2nd generation lentiviral vector, in addition to pCDH CMV MSCV E2F1GFP expression vector. The pCDH CMV MSCV E2F1GFP vector did not function well during cloning so the predominantly used vector became FoxJ1-IRESEGFP. This lentiviral vector had a backbone size of approximately 10 kb and contained a *SfiI* cloning site upstream of the EF1α promoter. The *SfiI* cloning site included two specific *SfiI* cleavage sites that allowed for controlling the insert's orientation into the vector. Additionally, IRES2 (Internal Ribosome Entry Site 2) and EGFP (Enhanced Green Fluorescent Protein) sites were located in the sequence of this vector. IRES2 permits increased expression and translation of the reporter gene (EGFP) in the bicistronic transcript of the lentiviral construct. By containing both the EF1α promoter and IRES2, FoxJ1-IRESEGFP allowed for co-expression of the particular STAT3 insert and EGFP, which facilitated selection of transfected and transduced cells (*SBI: Systems Bioscience* User Manual, 2012). The general structure of this vector is shown in Figure 2.

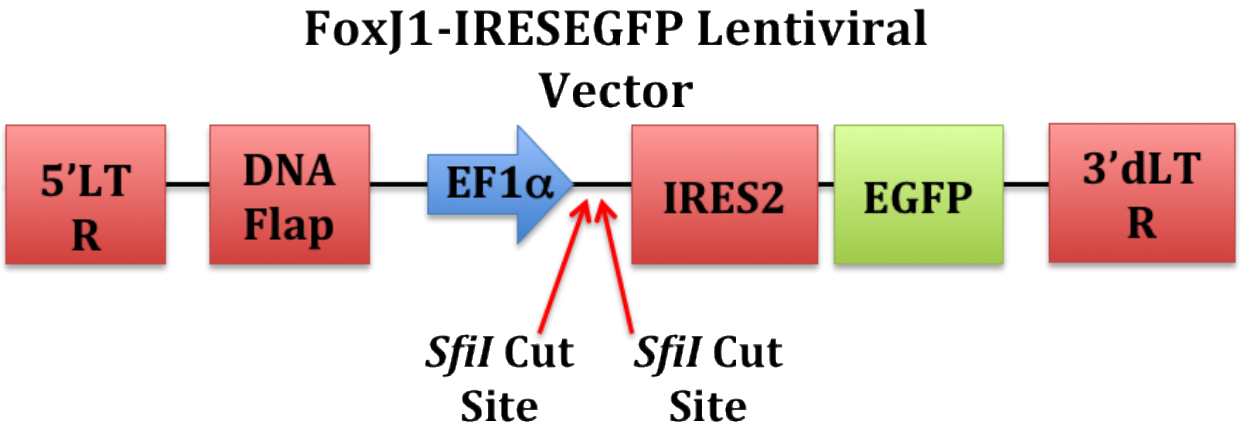

Figure 2: *General structure of the FoxJ1-IRESEGFP lentiviral expression plasmid in which STAT3 WT, STAT3 Y705F, STAT3 CC, STAT3 EE, and STAT3 VVV were cloned.* The lentiviral vector sequence contains a 5'LTR, a DNA flap, an EF1α promoter, a *SfiI* cloning site containing two *Sfi*I cleavage sites, IRES2, EGFP, and a 3'dLTR. The FoxJ1-IRESEGFP lentiviral vector has a backbone size of approximately 10 kb and the *SfiI* cloning site is located directly upstream of the EF1α promoter sequence. STAT3 inserts were cloned into the vector immediately upstream of the EF1 promoter sequence, creating a bicistronic construct including the insert and EGFP. STAT3 genes themselves were not tagged with GFP, and thus, GFP expression came from the vector that the inserts were cloned into. The lentiviral vector was donated by Iyor Lemischka (Mount Sinai Medical Center, NY).

The STAT3 Y705F and STAT3 CC mutant cDNAs were originally cloned into pRC/CMV vectors, the STAT3 EE and STAT3 VVV mutants were cloned into TOPO vectors and the STAT3 WT cDNA was cloned into a pCMV-HA-tagged vector. In order to clone each STAT3 gene into a FoxJ1-IRESEGFP lentiviral vector, PCR amplification was used to generate the individual STAT3 gene fragments. PCR amplification was performed using PCR10 and PCR11 primers containing a DNA sequence specific for the *SfiI* restriction enzyme. The PCR amplification products generated with each STAT3 plasmid were treated with *DpnI* restriction enzyme to digest all methylated DNA and leave only the cDNA of each STAT3 gene with a *SfiI* cleavage site on either side of the STAT3 insert. The five STAT3 cDNAs and the FoxJ1-IRESEGFP vector were digested with *SfiI* restriction enzyme. *SfiI* digestion resulted in generation of sticky ends (overhangs) on both the vector and the STAT3 cDNAs; these overhangs supported proper annealing of the inserts into the FoxJ1-IRESEGFP vector during ligation. Ligated lentiviral plasmids were transformed into TAM1 *E. coli* cells and these bacterial cells were grown on LB+agar plates. Bacterial colonies were screened for the presence of individual lentiviral plasmids by PCR; about twelve colonies from each transformed bacterial plate were tested, and several positive clones were obtained. When run on a 1.6% agarose gel, the PCR positive plasmids exhibited a band with a correct size of about 200 bp correlating with the STAT3 insert [Figure 3].

Selected bacteria were expanded to produce larger amounts of plasmid DNA (midipreps). The Midipreps typically produced 50 – 200 ug of DNA at a final concentration of approximately 0.25 – 1.0 ug/ul per lentiviral construct. A similar amount of DNA was obtained for the isolated FoxJ1-IRESEGFP lentiviral vector using the same procedure. Digesting each construct with *SfiI* and comparing the results to undigested constructs confirmed proper insertion of the STAT3 gene. The five STAT3 lentiviral plasmids were obtained.

PCR Screening of TAM1 Bacterial Cells Cloned with the STAT3 CC Lentiviral Construct

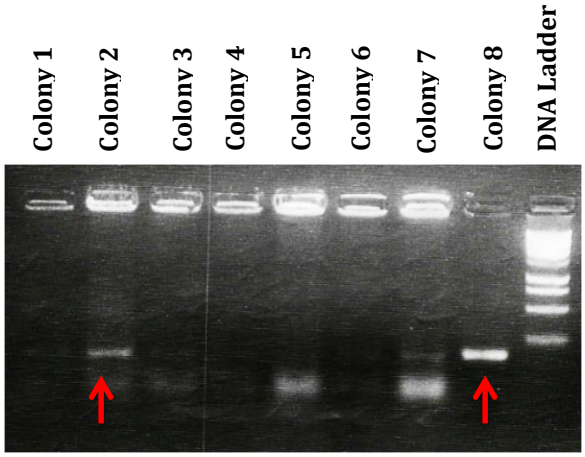

Figure 3: *PCR screening of TAM1 E. coli cells transformed with STAT3 CC lentiviral construct.* 8 colonies were PCR screened to decipher which colonies were successfully cloned (positive for recombination). Both colonies 2 and 8 expressed a band of about 200 bp in length demonstrating that the STAT3 insert was successfully cloned into these colonies. Each positive colony was grown to produce more of the lentiviral construct necessary for lentiviral production; this was performed for all lentiviral STAT3 plasmids.

Production of Lentiviruses Encoding STAT3 WT and STAT3 Mutants

The purpose of cloning the STAT3 inserts into a lentiviral plasmid vector was to generate virus that could be used for stable integration and expression of STAT3 WT and STAT3 mutant genes in cell genomes. The production of lentiviruses is presented diagrammatically in Figure 4. Separate plates of HEK-293T cells cultured in DMEM medium were transfected with each of the five STAT3 lentiviral constructs with two specific lentiviral packaging plasmids, psPax2 and pMD2.G. Transfected cells were viewed by fluorescent microscopy to detect viral GFP and gauge the effectiveness of transfection. Following plasmid transfection, lentiviruses were collected in the media (36-39 hours post-transfection). Lentiviruses were collected on three separate occasions, each twelve hours apart, and stored as small aliquots. HEK-293T cells were approximately 80-90% confluent at this point and roughly 50-60% of the cells were fluorescent and positive for GFP expression (Figure 5). This was an indication that the STAT3 lentiviral constructs had entered the cells and lentiviral production had begun (Figure 5).

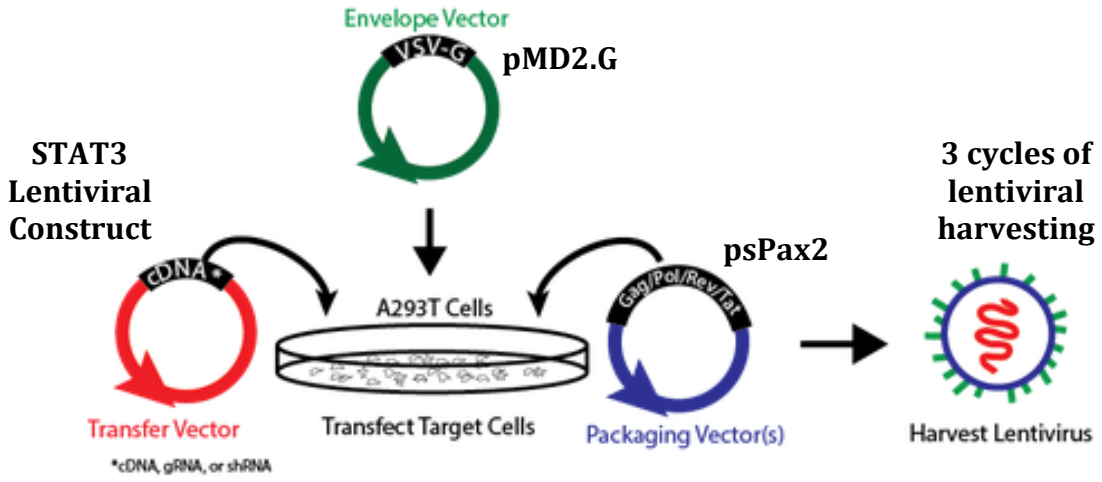

Figure 4: *Lentiviral production diagram obtained from Addgene (Lentiviral Guide – Viral Production).* The diagram shows a general scheme of generating lentiviruses beginning with transfection of HEK-293T cells with the enveloping plasmid/vector (pMD2.G), the packaging plasmid/vector (psPax2), and the transfer vector (STAT3 lentiviral plasmid). pMD2.G contains a VSV-G tag and psPax2 includes genes that encode for the major (HIV) viral structural proteins (Gag, Pol, Rev, and Tat). Collection of lentiviruses begins approximately 1.5 days after the initial transfection and is done a total of three times with each harvesting event being 12 hours apart.

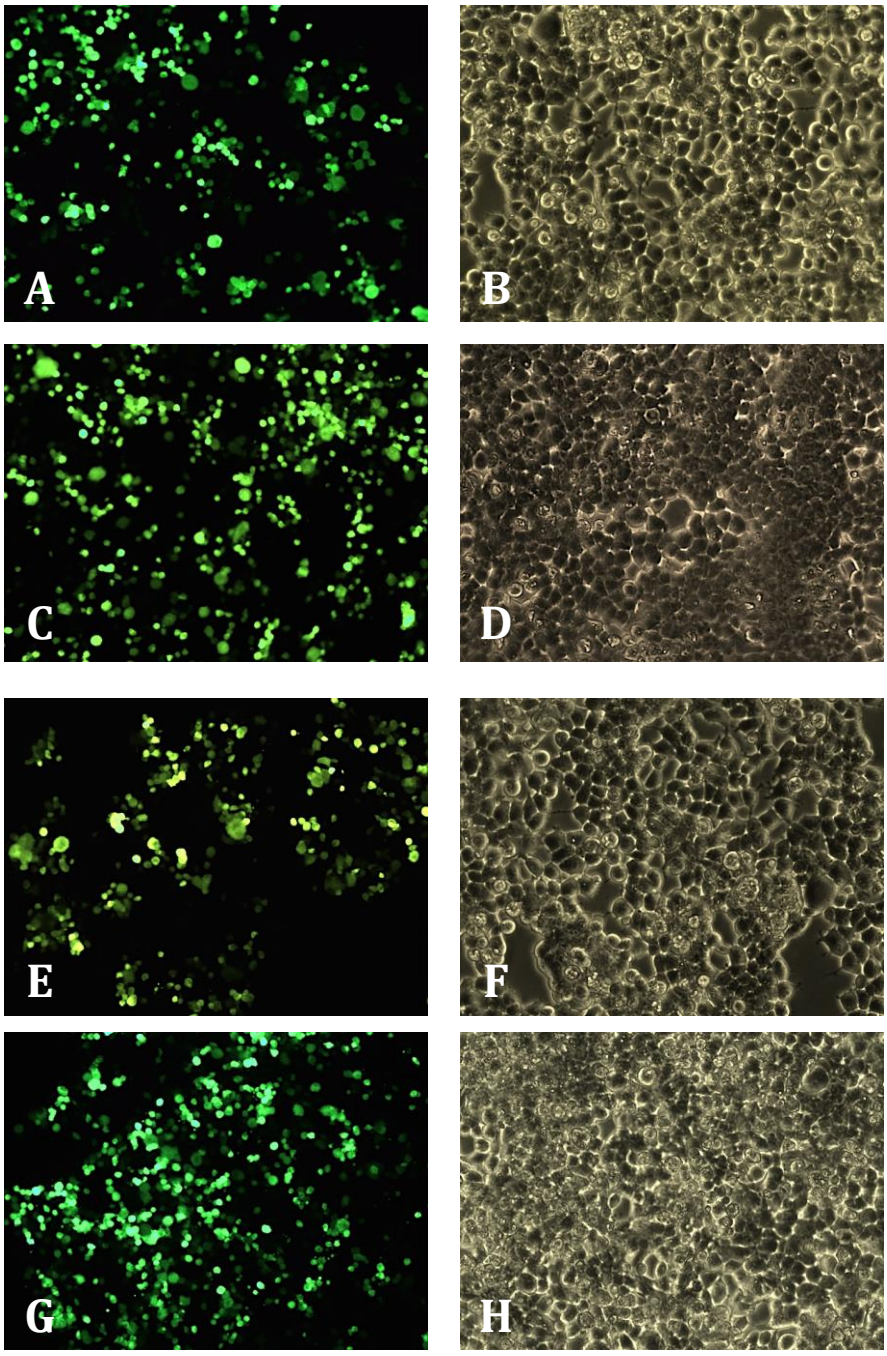

Figure 5: *HEK-293T cells transfected with lentiviral plasmids.* STAT3 WT (A and B), STAT3 Y705F (C and D), STAT3 CC (E and F), and STAT3 EE (G and H). Images A, C, E, and G portray GFP expression of transfected HEK-293T cells. Images B, D, F, and H portray HEK-293T cells under white light (without fluorescence). Similar results were obtained from transfections with STAT3 VVV, although not pictured here.

Lentiviral Transduction of HeLa Cells With STAT3 Lentiviral Constructs

The medium from HEK-293T cells transfected with the lentiviral plasmids contained the produced lentiviruses and this media was harvested for use in infections. Media with STAT3 lentiviruses were pipetted onto HeLa cells (50-80% confluent) for transduction; this was done to permanently incorporate the various STAT3 inserts (WT and mutants) into the genomes of infected cells to overexpress each STAT3 construct with respect to endogenous levels of STAT3. 48 hours after lentiviral infection, the transduction efficiency was determined by fluorescent microscopy (Figure 6). Based on cellular fluorescence, a viral titer of the harvested lentiviruses was estimated. By two days post-infection, cells were assessed to be about 50-60% fluorescent, giving a good indication that 50-60% of cells were successfully infected by the STAT3 lentiviral construct(s).

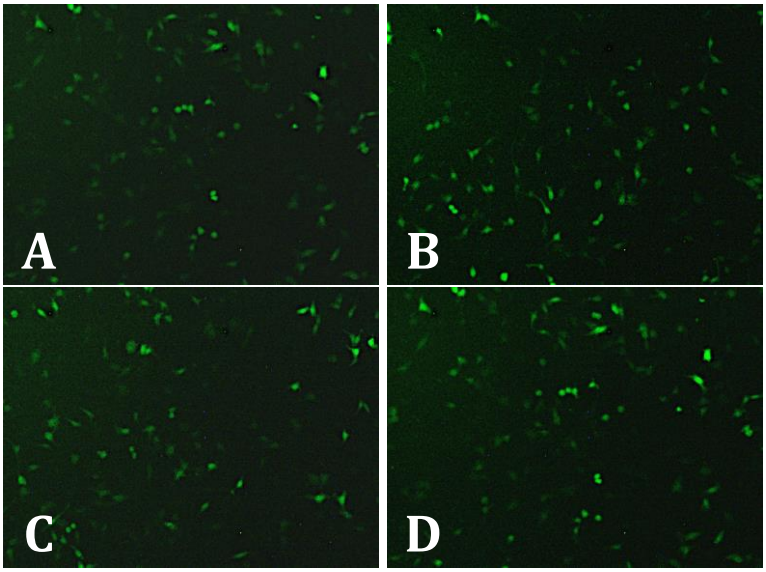

Figure 6: *Images of fluorescent HeLa cells infected by four STAT3-expressing lentiviruses.* HeLa cells infected with lentiviral constructs including (A) STAT3 WT, (B) STAT3 Y705F, (C) STAT3 CC, and (D) STAT3 EE. Images were taken approximately two days after infection; cells were treated with 6 ul of lentiviral solution each. Infections with STAT3 VVV lentiviruses were also done (not pictured) and resulted in a similar fluorescence efficiency of about 50-60% of HeLa cells in

Western Blots to Measure Expression of STAT3 in Lentiviral-Infected Cell Lines

GFP fluorescence is a marker for transfection or infection of cells with the FoxJ1-IRESEGFP lentiviral vector, but it does not necessarily indicate that the particular STAT3 insert (cloned into the vector) was taken up by the cells and integrated into their genomes. To view the extent to which infection increased STAT3 expression in infected HeLa cells, protein lysates were made and the proteins were used to produce Western blots. Western blots showed predictable elevated levels of STAT3 in the STAT3 WT, STAT3 Y705F, STAT3 CC, STAT3 EE, and STAT3 VVV infected cells with respect to vector-infected (FoxJ1-IRESEGFP) cells (data not shown). MAPK (ERK1/2) expression was used as a loading control and appeared uniform and of equal intensity in all infected cells. The results allowed for a better estimation of the viral titer for each STAT3 lentiviral solution.

After the lentiviruses were produced and tested, the objective was to infect various cells with these lentiviruses to evaluate the effects of increased expression of either STAT3 WT or one of the four mutant STAT3 genes. Several different cell lines were transduced including MCF10A cells (human breast/mammary epithelial cells), MEF cells (Murine Embryonic Fibroblasts), murine pancreatic cells, and murine lung cells. Flow cytometry analysis was performed by Alexei Petrenko to determine how many cells were successfully infected. Shown in Figure 7 are the results obtained from flow cytometry analysis of MCF10A cells infected with STAT3 WT, STAT3 CC, and STAT3 Y705F. Results showed that roughly 60-70% of MCF10A cells (non-tumorigenic human breast epithelial cells) were fluorescent; flow cytometry was performed on all of the infected cell lines studied, and the results were similar in all cases. Western blots conducted by Alexei Petrenko indicated an increase in STAT3 expression of all infected cell lines following infection (Figure 8). In contrast, empty vector infected cells exhibited much lower levels of STAT3 representing endogenous STAT3 expression (Figure 8). Shown in Figure 8 is one of the Western blots performed using protein lysates obtained from p53 -/- MEFs (expressing the KRAS mutation; Ischenko, Zhi, Moll, *et al* 2013) infected with each of the vector or STAT3 constructs; this procedure was done on all infected cell types and the results showed increased levels of STAT3 in cells infected with STAT3-containing lentiviruses in comparison to vector-infected cells, as expected. This was another verification that infections worked properly and the lentiviruses produced did contain the necessary STAT3 cDNAs.

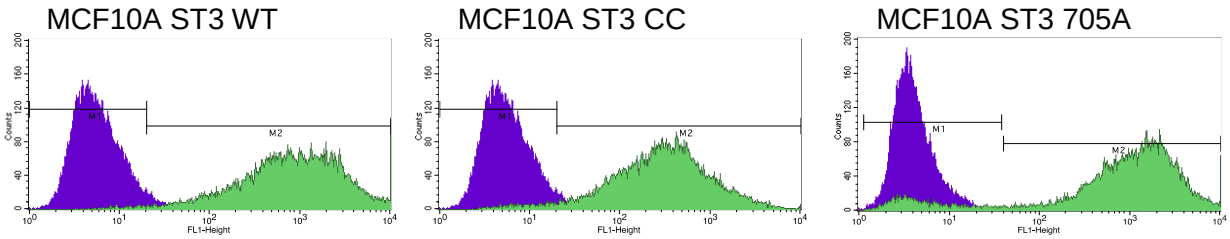

Figure 7: *Flow cytometry analysis of MCF10A human breast epithelial cells infected with WT, CC, and Y705F STAT3 lentiviral constructs, approximately two weeks post-infection.* The *x*-axis (horizontal axis) indicates the FITC intensity; this is the intensity of GFP fluorescence in the population of cells. The *y*-axis (vertical axis) shows the detected number of cells that experience a particular strength of fluorescence. These results showed that roughly 50-60% of cells infected with STAT3 WT, STAT3 CC, and STAT3 Y705F exhibited fluorescence (green) with respect to the control group (measured and documented in purple). FACS analysis was performed similarly on all populations of infected cells studied, and with all five STAT3 lentiviral constructs prior to performing Western blots. Flow cytometry analysis (FACS) was conducted by Alexei Petrenko.

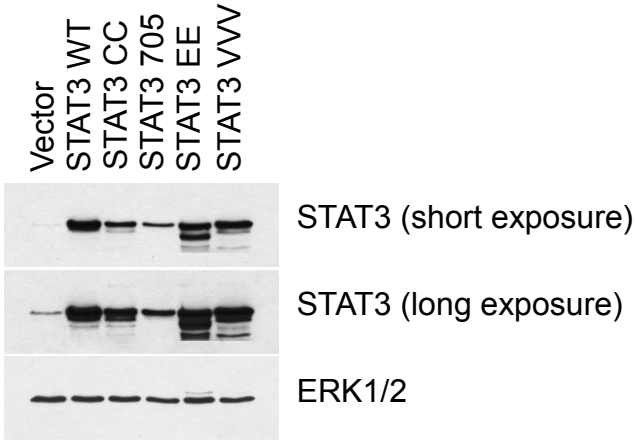

Figure 8: *Western blot of p53 -/- MEFs with endogenous mutant K-RasG12D infected with vector (control), STAT3 WT, STAT3 CC, STAT3 Y705F, STAT3 EE, and STAT3 VVV.* Expression levels were taken under both a short exposure and a long exposure. Based on this information, lentiviral infection was successful and the results showed increased total STAT3 expression in all MEFs infected with STAT3-containing lentiviral constructs. Vector-infected MEFs exhibited lower levels of STAT3, reflecting endogenous levels of STAT3 in this cell line. ERK1/2 (MAPK) expression is shown as a loading control marker. Similar Western blots were carried out with each cell line used, showing comparable results to what was seen here (increased STAT3 expression when STAT3-containing lentiviruses were used for infection). Western blot produced by Alexei Petrenko.

Altered Tumor Growth Rates and Phenotypes of Nude Mouse Xenographs Expressing Lentiviral STAT3

Once it was established and verified that all cell lines were expressing the correct lentiviral construct, *in vivo* studies were carried out on nude mice to ascertain how overexpression of particular STAT3 constructs affected tumorigenesis (tumor growth rate and tumor histology). About 10,000 cells of each cell type infected with a particular lentiviral construct was injected into four quadrants of a single nude mouse, at locations adjacent to the shoulder of every limb, and tumors were left to develop for several months. Injections were performed with pre-malignant (p53-/-; K-RasG12D) murine pancreatic cells (clones 2 and 16) and pre-malignant (p53-/-; K-RasG12D) murine lung cells (clones 8 and 28) infected with STAT3 WT, STAT3 CC, and STAT3 EE lentiviruses. Experiments with other cell types and infections with STAT3 Y705F and STAT3 VVV are still in preliminary stages awaiting tumor growth and development.

Pancreas 2 and 16 clonal cells expressing lentiviral STAT3 WT produced tumors more rapidly than cells expressing lentiviral STAT3 CC, STAT3 EE, or vector (Figure 9A). Vector-expressing cells developed tumors at about the same rate as cells with ectopic STAT3 EE expression as well as produced tumors with equal volumes (0.2 cm^3 at 24 days post-injection) at each time interval (Figure 9A). In both cases, ectopic expression of STAT3 CC resulted in a slight lag in tumor development rate relative to tumors produced by vector-infected cells, but this was not statistically significant (Figure 9A). Lung 8 and lung 28 clones expressing lentiviral STAT3 WT resulted in tumor development becoming severely delayed with respect to cells overexpressing vector (Figure 9B). STAT3 EE and vector overexpressing tumors grew at about the same rate in both lung clones within the same timeframe. Lung 8 clone cells expressing lentiviral STAT3 CC yielded a delay in tumor development, however it was not quite as prominent as the delay associated with lentiviral STAT3 WT overexpression (Figure 9B); this delay was nonexistent during tumor development from Lung 28 clone cells overexpressing STAT3 CC (data not shown).

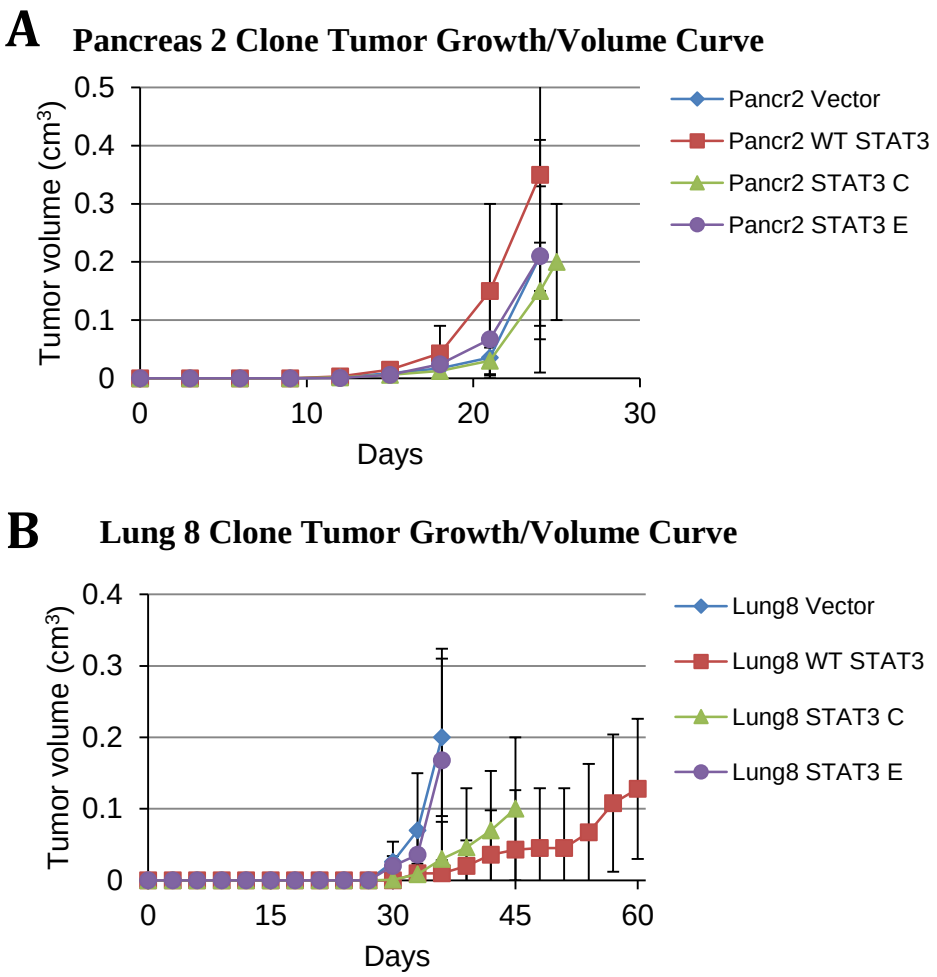

Figure 9: *Tumor volume curves generated from both infected Lung 8 clone cells and infected Pancreas 8 clone cells with FoxJ1-IRESEGFP vector, STAT3 WT, STAT3 CC, and STAT3 EE lentiviral constructs*. (A) *Pancreas 8 clone infected cells*: STAT3 WT overexpression resulted in an increased rate of tumor growth. STAT3 CC overexpression and STAT3 EE overexpression resulted in very slight changes in tumor growth. STAT3 CC overexpression caused a slight delay in tumor growth. (B) *Lung 8 clone infected cells*: Cells with STAT3 EE overexpression mimicked vector-infected cells, STAT3 CC and STAT3 WT overexpression resulted in delayed tumor growth, and STAT3 WT overexpression slowed down tumor growth and progression the most. Similar results were seen in tumors produced by infected Pancreas 16 clone cells and infected Lung 28 clone cells, respectively, although they are not shown. Growth curves were produced by Alexei Petrenko.

Tissue Histology of Tumors From STAT3 WT and STAT3 Mutant Infected Lung and Pancreas Clones are Distinct

To better understand the role of STAT3 in tumor development, the histology of each tumor was examined utilizing H&E and immunohistochemical staining. Using this information, the cellular structure and organization of the tumors were compared to identify if STAT3 WT or STAT3 mutant overexpression in a particular cell type/lineage (lung or pancreas clones) affects the predisposition of those cells to develop into a certain cancer type, or if there is an effect on the morphology of the tumors based on WT or mutant STAT3 overexpression.

Pancreas clone 2 and 16 tumors infected with STAT3 WT resulted in adenocarcinoma (ADC) phenotypes. ADC is characterized by glandular structures distinctly seen in images B and F of Figure 10. This is a stark contrast to the sarcomatoid carcinoma phenotype exhibited by tumors derived from pancreatic clonal cells overexpressing empty vector (Figure 10 A and E). The ADC phenotype promoted by WT STAT3 was more prominent in clone 2 tumors overexpressing STAT3 WT than clone 16 tumors. Moreover, STAT3 WT overexpression in clone 2 tumors resulted in much greater cell death, as indicated by large quantities of cell fragments, than in clone 16 tumors overexpressing STAT3 WT and in other tumors overexpressing other STAT3 mutants. Tumors from both pancreatic clones overexpressing STAT3 CC and STAT3 EE have an ADC phenotype present to a lesser degree than in clones overexpressing STAT3 WT (Figure 10 C&D, G&H). Glandular structures are still present however they are not as abundant throughout the tumors' composition. This glandular (ADC) phenotype is stronger in tumors originating from infected clone 2 cells as opposed to tumors from infected clone 16 cells.

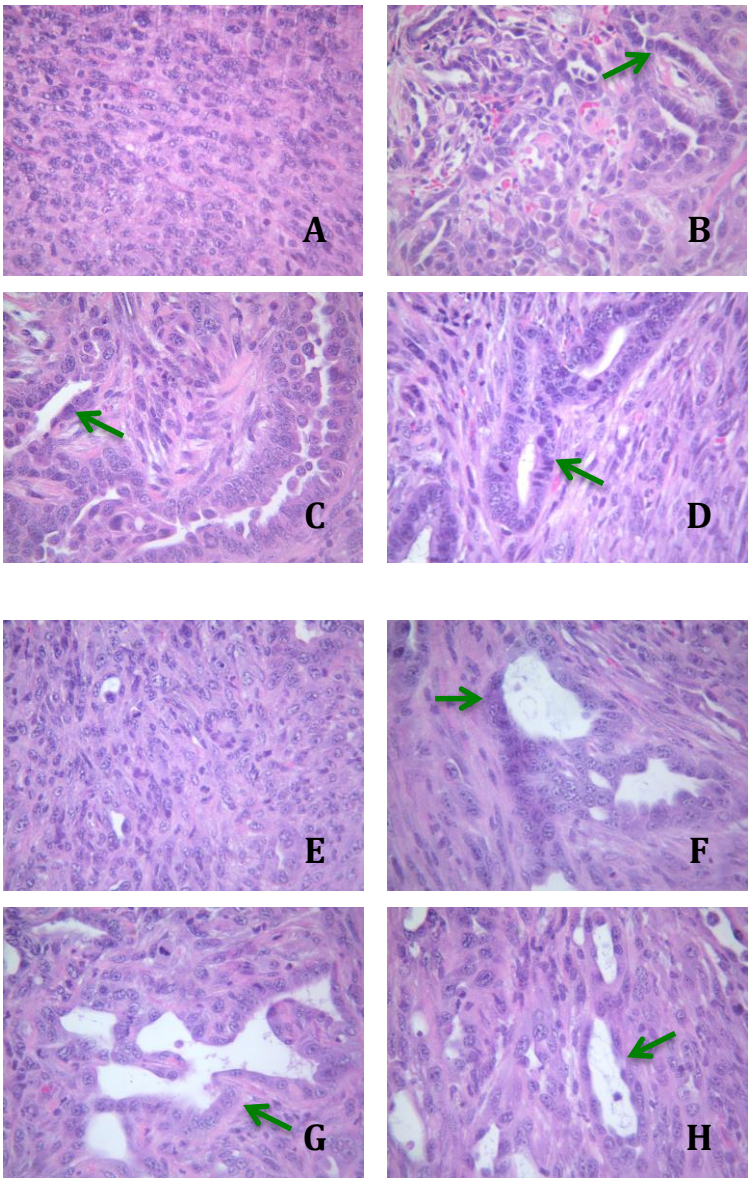

Figure 10: *H&E staining of tumor sections from infected pancreas clone 2 and 16 cells; images (40x magnification) A-D are tumor sections derived from pancreas 2 clonal cells whereas E-H are tumor sections from pancreas 16 clonal cells.* Tumor derived from pancreas 2 clonal cells overexpressing (A) FoxJ1-IRESEGFP vector, (B) STAT3 WT, (C) STAT CC, and (D) STAT3 EE. Tumor derived from pancreas 16 clonal cells overexpressing (E) FoxJ1-IRESEGFP vector, (F) STAT3 WT, (G) STAT3 CC, and (H) STAT3 EE. Green arrows point towards ADC morphology and ductal structures seen in the tumor sections/samples.

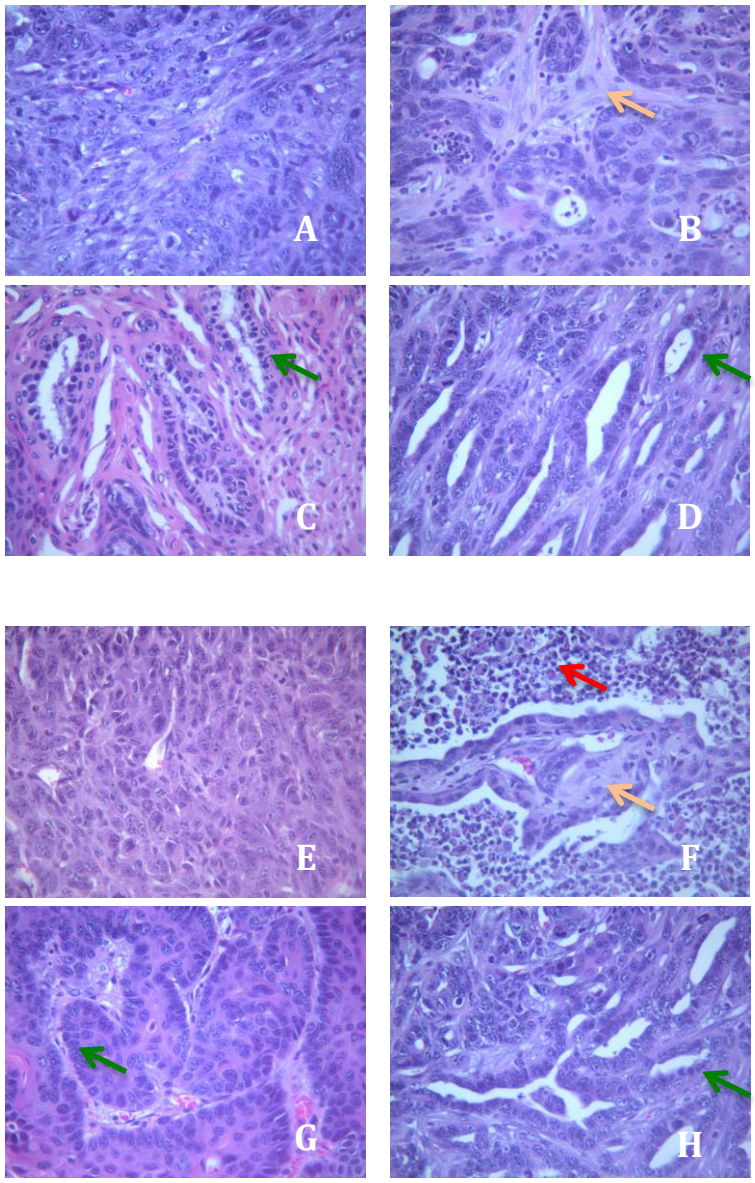

Figure 11: *H&E staining of tumor sections from infected lung clone 8 and 28 cells; images (40x magnification) A-D are tumor sections taken from lung 8 clone tumors; images E-H are tumor sections taken from lung 28 clone tumors.* Tumor derived from lung 8 clonal cells overexpressing (A) FoxJ1-IRESEGFP vector, (B) STAT3 WT, (C) STAT3 CC, and (D) STAT3 EE. Tumor derived from lung 28 clone cells overexpressing (E) FoxJ1-IRESEGFP vector, (F) STAT3 WT, (G) STAT3 CC, and (H) STAT3 EE. Green arrows show ductal (ADC) morphology, red arrows indicate dead cells and cellular debris dispersed with infiltrated leukocytes, and the orange arrows point to examples of SCC morphology.

Overexpression of STAT3 WT in lung clone 8 and 28 cells resulted in tumors that developed into squamous cell carcinomas (SCC). Images B and F (Figure 11) show large

quantities of tumor cells forming flat, track-like structures that indicate SCC morphology. This is in constrast to vector overexpression in these clones that leads to a sarcomatoid carcinoma phenotype as seen in images A and E (Figure 11). STAT3 WT overexpression also lead to a large population of dead cells in lung clone 8 and 28 tumors, which is seen by the abundance of small, cellular fragments scattered throughout the samples (Figure 11 B and F). Additionally, STAT3 WT overexpression (lung 8 and 28 tumor – Figure 11 B and F) also depicts large-scale leukocyte permeation indicating an inflammatory response/reaction had occurred. Lung 8 and 28 clones overexpressing STAT3 CC and STAT3 EE developed SCC morphologies as well, with the distinction that STAT3 EE overexpression gave rise to glandular structures separated by sections of squamous cell carcinoma (Figure 11 C and D; Figure 11 G and H); observations from a larger field show that STAT3 EE overexpression (lung 8 tumors) results in an adenosquamous tumor morphology (Figure 12D) that is not present when STAT3 CC levels are elevated (Figure 12C). Other fields showed that high levels of STAT3 EE expression in lung 8 and 28 clonal cells produced tumors with regions of SCC, ADC, and adenosquamous carcinoma morphology (data not shown).

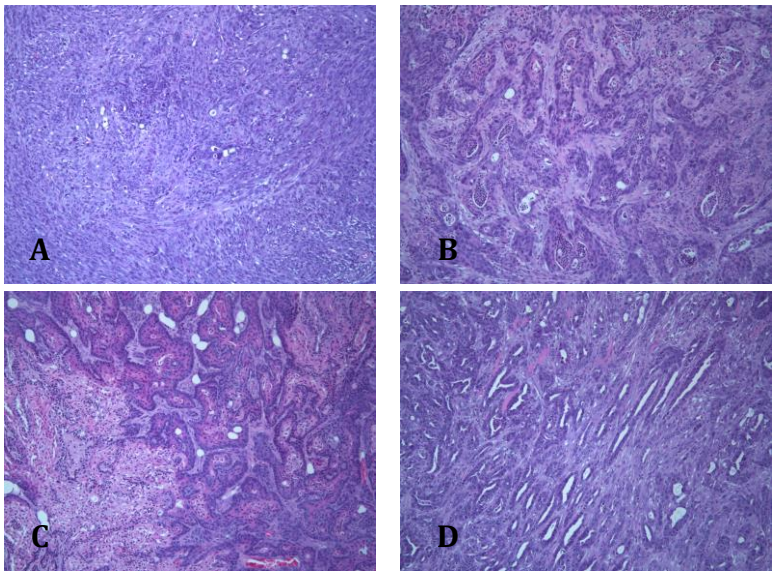

Figure 12: *10x magnification (larger field) of tumors derived from lung 8 clone cells infected with various lentiviral constructs.* Tumor overexpression of (A) FoxJ1-IRESEGFP vector, (B) STAT3 WT, (C) STAT3 CC, and (D) STAT3 EE.

To further analyze each tumor section, immunohistochemistry (IHC) was performed using markers for adenocarcinoma and squamous cell carcinoma phenotypes. Keratin 19 staining was used as a marker for SCC morphology in lung tumors and ADC morphology in pancreatic tumors (Dabeva, *et al* 1997; Abbas, *et al* 2011). IHC with keratin 19 showed definite SCC morphology in lung tumors with ectopic STAT3 WT expression when compared to tumors containing empty lentiviral vector (Figure 13 IC and ID). Keratin 19 staining of pancreatic tumor sections further distinguished the ductal (ADC) structures from surrounding tumor tissue. The ADC histology was much more prominent in pancreatic tumors overexpressing STAT3 WT than in tumors expressing empty vector (Figure 13 IIC and IID). Other stainings with antibodies for p63 and *beta*-catenin were also used to observe the extent and divergence of tumor differentiation (data not shown). All immunohistochemical stainings verified the presence of specific tumor morphologies and proved the histological classifications to be accurate. IHC will be performed on tumors derived from other transduced cell lines once the experiments are completed.

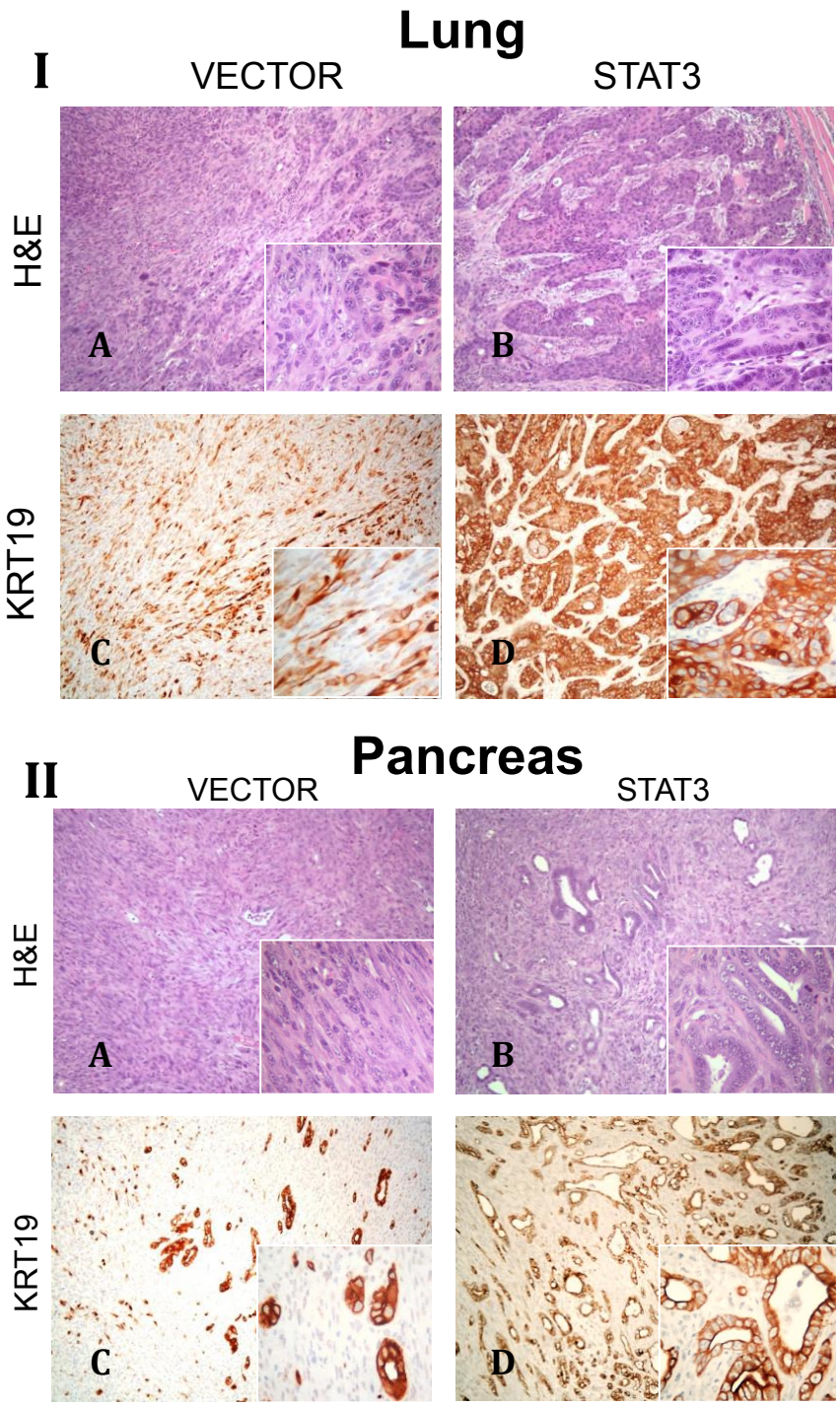

Figure 13: *[I] Images of lung tumor sections at 10x and 40x magnification after H&E and IHC staining.* Images show morphology of vector-expressing lung tumors stained via (A) H&E and (C) keratin 19 staining, as well as ectopic STAT3 WT-overexpressing lung tumors stained with (B) H&E and (D) keratin 19 staining. *[2] Images of pancreatic tumor sections at 10x and 40x magnification after H&E and IHC staining.* Morphology of vector-expressing pancreatic tumors stained with (A) H&E and (C) KRT19 staining, in addition to STAT WT-overexpressing pancreatic tumors stained with (B) H&E and (D) KRT19 staining. Other IHC stainings were done using *beta*-catenin and p63, although not shown.

Chapter 4

Discussion

Parallel to other transcription factors, STAT3 functions by translocating into the nucleus, binding to promoter regions of specific genes and initiating transcription. Activated STAT3 is responsible for expression of a number of genes involved in cell proliferation, cell growth, survival, and differentiation (Hirano, Ishihara, and Hibi, 2000). Altered IL-6/JAK/STAT3 signaling has been correlated with tumorigenic phenotypes in cells that ultimately develop into cancer. As mentioned earlier, mutations that cause hyperactivation of tyrosine kinases (JAK, c-Src, EGFR, etc.) upstream in the STAT3 signaling pathway can result in constitutive activation of STAT3 (Frame, 2002; Gao, *et al* 2007; Oku, *et al* 2010). STAT3 can also become constitutively activated in response to defects and negative mutations of certain phosphatases whose purpose is to regulate STAT3 activation (Irie-Sasaki, *et al* 2001; Han, *et al* 2006; Bard-Chapeau, *et al* 2011). Moreover, mutations in the STAT3 protein itself can greatly impact the JAK/STAT signaling pathway, particularly in amino acid residues essential for proper activation, dimerization, and DNA binding; these STAT3 mutations are rare but are most frequently seen in hematopoietic malignancies (Couronné, L., *et al* 2013). Many cancers that exhibit changes in STAT3 signaling rely on the defective properties of one of these components in the signaling mechanism. However, specific mutations to the pathway affect different cell types in numerous ways that can either promote or inhibit tumor development. Our research focused on how several key mutations (negative/inhibitory mutations and activating mutations) in the STAT3 protein affect cellular growth characteristics, tumor development, and tumor morphology when these STAT3 constructs are ectopically expressed in various (pre-malignant) cell lines containing oncogenic K-RasG12D. STAT3 DNA-binding mutants, constitutively dimerized/active mutants, and inactive tyrosine mutants were used to demonstrate how overexpression of hyperactive or inactive STAT3 constructs could compare to the phenotype obtained from endogenous STAT3 expression. The goal was to better describe the significance of STAT3 in pre-malignant cells, STAT3's cooperation with oncogenic proteins (such as K-RasG12D), and STAT3's role in tumorigenesis.

By generating lentiviruses containing STAT3 WT or one of the four STAT3 mutants, we were able to successfully overexpress each STAT3 gene in populations of pre-malignant (p53-/- and oncogenic K-RasG12D) lung cells and pre-malignant (p53-/- and oncogenic K-RasG12D) pancreatic cells, inject these transduced cells into nude mice, and observe tumor formation and growth. Tumors were then H&E stained as well as treated with immunohistochemical stainings for keratin 19, p63, and *beta*-catenin to compare histological and morphological phenotypes.

STAT3, and the IL-6/JAK2/STAT3 signaling pathway as a whole, has been reported to influence oncogenic K-Ras-induced pancreatic tumorigenesis (Corcoran, *et al* 2011). Studies have found that phosphorylated and activated STAT3 plays a large role in pancreatic tumor initiation as well as the progression of pancreatic tumors from lesions (pancreatic intraepithelial neoplasias and acinar-to-ductal metaplasias) to invasive, highly differentiated pancreatic ductal adenocarcinomas (Corcoran, *et al* 2011). Mainly, active STAT3 appears to be a driver for continued proliferation of pancreatic pre-malignant cells within many of these early lesions that eventually develop into more severe morphological structures (Corcoran, *et al* 2011). Because of this described link between activated STAT3 and pancreatic tumor progression and pathogenesis, we aimed to overexpress various STAT3 constructs in several clones of pancreatic cells to evaluate how loss-of-function or gain-of-function STAT3 can influence tumorigenesis. We predicted that constitutive activation of STAT3 by means of overexpression of STAT3 CC would hasten tumor development and exacerbate the ductal (ADC) morphology seen in tumors produced from transduced pancreatic cells, whereas overexpression of STAT3 EE (a negative, DNA binding mutant) would decrease tumor development/growth rates and result in less differentiated tumor morphology. Our data showed relatively little change in tumor growth rate between tumors grown from STAT3 CC-infected pancreatic cells and STAT3 EE-infected pancreatic cells (of various clones); both mutations also resulted in enhanced formation of ductal structures (ADC phenotype) in tumors with respect to vector-transduced tumors (Figures 9A and 10). The strongest phenotype was seen from ectopically expressing STAT3 WT; increased levels of STAT3 WT mildly accelerated tumor development (Figure 9) while also yielding the most pronounced ductal/ADC morphology (Figure 10). These results were equivalent between tumors derived from two individual clones of pancreatic cells. The results obtained from STAT3 WT overexpression seem to correlate with recent findings of STAT3 involvement in pancreatic

tumorigenesis, however there are noticeable disparities between predicted and acquired outcomes utilizing overexpression of STAT3 CC and STAT3 EE mutants.

In regards to lung cancer, STAT3 has been portrayed as having opposing roles in tumor progression depending on the upstream mutations in signaling cascades and lung cell types in which the tumor originates from. In lung cells with oncogenic K-RasG12D, STAT3 functions as a tumor suppressor that inhibits growth and advancement of lung adenocarcinomas (Grabner, *et al* 2015). Many lung tumors that express oncogenic K-RasG12D also express low levels of STAT3, further validating that STAT3 is essential for prevention of lung adenocarcinoma development and loss of STAT3 enhances this tumorigenic phenotype (Grabner, *et al* 2015). We assessed tumor growth and morphology from two clonal populations of lung cells containing oncogenic K-RasG12D when overexpressing STAT3 WT or one of the STAT3 mutants (CC and EE). Tumors overexpressing STAT3 WT (derived from both lung clones) displayed a squamous cell carcinoma morphology that contained significant necrosis (cell death) and leukocyte penetration (Figure 11 B and F). Necrosis on this scale was not seen in any other tumor derived from STAT3 CC or STAT3 EE transduced pre-malignant lung cells. STAT3 EE overexpression produced tumors that had sections of ADC, SCC, and adenosquamous carcinoma (ASC) morphology with formation of well-defined ductal structures (Figure 11 D and H), whereas STAT3 CC overexpression resulted in a predominantly SCC morphology (Figure 11 C and G). Differentiated tumor structures were distinguishable after H&E and IHC staining; markers for ductal and SCC morphologies were used as stainings to reinforce our conclusions. Antibodies for CD45 will be used to stain leukocytes in order to verify the inflammatory response seen when STAT3 WT is ectopically expressed. Thus, overexpression of a loss-of-function mutant STAT3 such as STAT3 EE, which inhibits DNA binding and transcription of downstream genes, is able to inactivate STAT3 function and result in more differentiated lung tumor development (into ADC – Figure 11 D and H; Figure 12D). These data correspond to previous literature that assigned tumor-suppressive properties to STAT3 in hyperactive K-Ras mutant lung cells/tumors (Grabner, *et al* 2015). Tumor growth rates also seemed to validate the conclusion that STAT3 is essential for repressing tumor development; STAT3 EE overexpression lead to the most rapid tumor growth, while STAT3 WT and STAT3 CC overexpression slowed tumor growth drastically (Figure 9B). It was assumed that STAT3 CC overexpression, introducing high levels of constitutively activated STAT3, would act to slow down tumor development the most in these

lung cells, however this was not what was detected. The noticeable increase in rate of tumor growth in tumors with ectopic expression of STAT3 EE compared to ectopic expression of STAT3 CC or STAT3 WT verifies that STAT3 is a necessary protein for slowing down tumorigenesis in certain lung cells/cancers.

In some cases, the mutations appear to function as expected, however certain instances showed results that countered what was originally anticipated. Because STAT3 CC is reportedly a constitutively activating mutant, it was expected that ectopic STAT3 CC expression would yield results similar to ectopic STAT3 WT expression except amplified to a higher degree. Unexpectedly, STAT3 CC failed to function as a true activating mutant construct as it did not produce a faster tumor growth rate or a more differentiated histological phenotype in pancreatic tumors. Furthermore, STAT3 CC did not generate a strong enough inhibitory effect on lung tumor development based on morphology and growth rate. Overexpression of STAT3 WT in lung tumors also produced a surprisingly extreme morphological phenotype provided that STAT3 has been assumed to inhibit tumor differentiation and progression in oncogenic K-Ras lung cells (Grabner, *et al* 2015).

It may be the case that cellular STAT3 concentrations are maintained within a specific range, and that cells are highly sensitive to changes in levels of STAT3. Recent studies have shown that once a particular threshold of STAT3 is reached and/or exceeded, cells shift from a self-renewing state to a differentiating state (Tai, Schulze, and Ying, 2014). STAT3 expression above a certain concentration appears to trigger a transition from promoting cell proliferation to promoting differentiation (Tai, Schulze, and Ying, 2014). Thus, by ectopically expressing WT STAT3 or different STAT3 mutants, this overall elevation in cellular STAT3 may have increased concentrations above the threshold, causing differentiation regardless of the specific ectopically expressed STAT3 construct. This may be the reason why STAT3 WT overexpression, in the particular lung cells studied, generated tumors with highly differentiated morphologies and severe immune responses, even when STAT3 WT has been said to play inhibitory roles in tumor progression.

It is important to note that mutant STAT3 proteins may be able to dimerize with other transcription factors, depending on the specific amino acid mutation. This would allow for regulation of different genes with regards to the concentration of particular mutant STAT3/transcription factor complexes. Recent findings state that NF-κB has the potential to

bind to unphosphorylated STAT3 (U-STAT3) (Yang, *et al* 2007). U-STAT3 competes with □κ□□for binding to NF-κB, with U-STAT3/U-NF-κB signaling resulting in activation of specific genes/oncogenes (*RANTES, IL-6, MET, RAS,* etc.) (Yang, *et al* 2007). Comparable to the well-known JAK/STAT pathway, this reflects another pathway in which STAT3 may function to increase cell growth and proliferation without homodimerizing or heterodimerizing to another STAT protein, and without phosphorylation for activation. If this is the case, then it may be possible that mutant STAT3 proteins, when ectopically expressed, dimerize with other transcription factors (similar to NF-κB) to regulate different sets of genes involved in tumorigenesis and tumor differentiation. In addition, the genes activated by U-STAT3/U-□F-κ□ signaling may promote increased expression of STAT3 that leads to higher levels of phosphorylated STAT3 (P-STAT3) and U-STAT3 (Yang, *et al* 2007), which can further amplify the effects of irregular STAT3 expression by feeding into both P-STAT3 and U-STAT3 signaling pathways. When coupled together in cells, these two different pathways begin functioning simultaneously to promote gene transcription and morphological changes in cells that lead to tumorigenesis (Yang, *et al* 2007). Ultimately, these data suggest how it is possible that ectopic STAT3 expression of any construct can affect further STAT3 expression in addition to perhaps playing one of several roles in gene transcription that can lead to cancer. Initially, it was believed that ectopic expression of certain STAT3 mutants would either promote or repress cell proliferation, cell growth, and survival, however based on the information we obtained, it appears as though a critical concentration of STAT3 can be reached/exceeded that results in a transition from a tumor promoting to tumor differentiating phenotype. This concentration-dependence was alluded to earlier when ectopic expression of all STAT3 mutants lead to a certain degree of morphological changes associated with tumor differentiation. This subject will be tested further once all STAT3 lentiviral constructs have been produced and administered to cells for tumor growth and analysis.

With all the work that has been done, many questions remain to be addressed. There are still several negative STAT3 mutants (Y705F – inactivating mutant, VVV – DNA binding mutant) that have yet to be completely examined; injections of ectopic STAT3 Y705F and STAT3 VVV expressing lung and pancreatic cells have been performed and the tumors have been excised, but further analysis (through IHC and H&E staining) has not been completed. Tumor growth (rate) curves will be constructed and histological analysis will be done on these

tumors to compare with histological data already obtained from the other STAT3 constructs. In addition, mutagenesis was performed to generate several other STAT3 mutants: STAT3 Y640F (gain-of-function mutant), STAT3 K658Y (hyperactive), and STAT3 S727E (activating/hypomorphic mutant). STAT3 S727E involves a mutation in a key serine residue that presumably increases the transcriptional activity of STAT3 by introducing a negatively charged amino acid (glutamic acid) that is involved in phosphomimicry (mimics phosphorylated serine residue) (Wen, Zhong, and Darnell Jr., 1995; Decker and Kovarik, 2000; Qin, *et al* 2008). STAT3 K658Y and STAT3 Y640F mutants contain mutations in the SH2 domain that are said to result in constitutively active (hyperactive) STAT3 proteins (Pilati, *et al* 2012). These activating and inactivating mutants can be used to compare with results obtained from STAT3 CC and STAT3 EE/STAT3 Y705F experiments, respectively, to better understand how hyperactivation or inactivation of STAT3 affects cell transformation and tumorigenesis. Lentiviruses will be produced using these STAT3 mutants and used for infection of various cell types (including the pancreas and lung clones). Additionally, focus will shift towards ectopic expression of all STAT3 constructs in other cell types. Similar to what was studied using the pancreas and lung cell clones, changes in cellular properties and tumorigenesis due to ectopic STAT3 (WT or mutant[s]) expression in MDA-MB-453 human breast cancer cells (containing catalytically active PI3K – PI3KCA-H1047R) will be observed using *in vitro* experiments (focus formation assays, suspension assays, soft agar assays, etc.) as well as *in vivo* following injections into nude mice, tumor growth rate observations, and assembling of tumor histological and morphological information. These will allow us to study the transformative properties of STAT3 (and mutant STAT3s) as well as STAT3's role in another cell line (breast cancer cell line) that is commonly affected by hyperactive STAT3 signaling. Once CRISPR-Cas9 is completed to knockout STAT3 in particular cell lines, these cells will be used to perform all STAT3 WT and mutant experiments again, without the presence of endogenous STAT3. This will provide more accurate information that is unhindered by normal expression of STAT3 in cells, which will permit us to effectively study how STAT3 functions within certain cells, and how each mutant STAT3 affects or alters cellular signaling (compared to WT or endogenous STAT3) to produce differences in tumorigenicity, tumor growth, and morphology. Lastly, human primary cancer cells (originating from pancreas, lung, breast tissue/mammary gland, etc.) will be treated with each STAT3 construct; primary cancer cells are derived directly from human donors (cancer patients) and

more closely mimic cancer cell properties and reproduction of cancer cell microenvironments that occur *in vivo* (in patients). Once everything is complete, the experiments will have to be redone several times to verify the conclusions. IHC staining for STAT3 will be performed to observe changes in STAT3 expression within each tumor section/sample.

In all, this research has the potential to offer great insight as to how STAT3 functions in different cell types to either promote or repress tumorigenicity, tumor progression, and transformation. By studying how ectopic expression of different STAT3 mutants affects tumor phenotypes from various cell types, one can learn a lot about how essential STAT3 is to a number of signaling pathways commonly defective in cancers, in addition to the importance of STAT3 concentration in comparison to significant mutations in the STAT3 structure when promoting tumor formation. A better understanding of the importance of STAT3 in certain human diseases and cancers can provide valuable information that may ultimately lead to the discovery of specialized drugs and treatments, and by ultimately observing how STAT3 affects primary cancer cells, it may be possible to personalize treatments for particular human cancers.

References

Abbas, O., Richards, J.E., Yaar, R., and Mahalingam, M. (2011). Stem cell markers (cytokeratin 15, cytokeratin 19 and p63) in *in situ* and invasive cutaneous epithelial lesions. *Modern Pathology*. **24:** 90-97.

Addgene. (2006). *pLKO.1 – TRC cloning vector: Producing lentiviral particles and infecting target cells*. Cambridge, MA. Addgene.

Addgene. (2006). *Lentiviral guide – Viral production*. Cambridge, MA. Addgene.

Argetsinger, L.S., Campbell, G.S., Yang, X., Witthuhn, B.A., Silvennoinen, O., Ihle, J.N., and Carter-Su, C. (1993). Identification of JAK2 as a growth hormone receptor-associated tyrosine kinase. *Cell*. **74(2):** 237-244.

Bard-Chapeau, E.A., Li, S., Ding, J., Zhang, S.S., Zhu, H.H., Princen, F., Fang, D.D., Han, T., Bailly-Maitre, B., Poli, V., Varki, N.M., Wang, H., and Feng, G.S. (2011). Ptpn11/Shp2 acts as a tumor suppressor in hepatocellular carcinogenesis. *Cancer Cell*. **19(5):** 629-639.

Bromberg, J. (2002). Stat proteins and oncogenesis. *J Clin Invest*. **109:** 1139-1142.

Bromberg, J., and Darnell Jr., J.E. (2000). The role of STATs in transcriptional control and their impact on cellular function. *Oncogene*. **19(21):** 2468-2473.

Bromberg, J.F., Horvath, C.M., Besser, D., Lathem, W.W., and Darnell Jr., J.E. (1998). Stat3 activation is required for cellular transformation by v-src. *Molecular and Cellular Biology*. **18(5)**: 2553-2558.

Bromberg, J.F., Wrzeszczynska, M.H., Devgan, G., Zhao, Y., Pestell, R.G., Albanese, C., and Darnell Jr., J.E. (1999). *Stat3* as an oncogene. *Cell*. **98(3)**: 295-303.

Corcoran, R.B., Contino, G., Deshpande, V., Tzatsos, A., Conrad, C., Benes, C.H., Settleman, J., Engelman, J.A., and Bardeesy, N. (2011). *STAT3* plays a critical role in *KRAS*-induced pancreatic tumorigenesis. *Cancer Res.* **71(14):** 5020-5029.

Couronné, L., Scourzic, L., Pilati, C., Della Valle, V., Duffourd, Y., Solary, E., Vainchenker, W., Merlio, J-P., Beylot-Barry, M., Damm, F., Stern, M-H., Gaulard, P., Lamant, L., Delabesse, E., Merle-Beral, H., Nguyen-Khac, F., Fontenay, M., Tilly, H., Bastard, C., Zucman-Rossi, J., Bernard, O.A., and Mercher, T. (2013). STAT3 mutations identified in human hematologic neoplasms induce myeoloid malignancies in a mouse bone marrow transplantation model. *Haematologica*. **98(11):** 1748-1752.

Dabeva, M.D., Hwang, S-G., Vasa, S.R.G., Hurston, E., Novikoff, P.M., Hixson, D.C., Gupta, S., and Shafritz, D.A. (1997). Differentiation of pancreatic epithelial progenitor cells into hepatocytes following transplantation into rat liver. *Proc Natl Acad Sci USA*. **94(14):** 7356-7361.

Darnell Jr., J.E., Kerr, I.M., and Stark, G.R. (1994). Jak-STAT pathways and transcriptional activation in response to IFNs and other extracellular signaling proteins. *Science*. **264:** 1415-1421.

De Souza, D., Fabri, L.J., Nash, A., Hilton, D.J., Nicola, N.A., and Baca, M. (2002). SH2 domains from suppressor of cytokine signaling-3 and protein tyrosine phosphatase SHP-2 have similar binding specificities. *Biochemistry*. **41(29):** 9229-9236.

Decker, T. and Kovarik, P. (2000). Serine phosphorylation of STATs. *Oncogene*. **19:** 2628-2637.
Frame, M.C. (2002). Src in cancer: deregulation and consequences for cell behaviour. *Biochim Biophys Acta*. **1602(2):** 114-130.

Friedlander, S.Y.G., Chu, G.C., Snyder, E.L., Girnius, N., Dibelius, G., Crowley, D., Vasile, E., DePinho, R.A., and Jacks, T. (2009). Context-dependent transformation of adult pancreatic cells by oncogenic K-Ras. *NCBI*. **16(5)**: 379-389.

Friedman, R.L., Manly, S.P., McMahon, M., Kerr, I.M., and Stark, G.R. (1984). Transcriptional and posttranscriptional regulation of interferon-induced gene expression in human cells. *Cell*. **38:** 745-755.

Gao, Y., Cimica, V., and Reich, N.C. (2012). Suppressor of cytokine signaling 3 inhibits breast tumor kinase activation of STAT3. *Journal of Biological Chemistry*. **287(25):** 20904-20912.

Gao, S.P., Mark, K.G., Leslie, K., Pao, W., Motoi, N., Gerald, W.L., Travis, W.D., Bornmann, W., Veach, D., Clarkson, B., and Bromberg, J.F. (2007). Mutations in the EGFR kinase domain mediate STAT3 activation via IL-6 production in human lung adenocarcinomas. *J Clin Invest*. **117(12):** 3846-3856.

Garcia, R. and Jove, R. (1998). Activation of STAT transcription factors in oncogenic tyrosine kinase signaling. *J Biomed Sci*. **5:** 79-85.

Garcia, R., Yu, C.L., Hudnall, A., Catlett, R., Nelson, K.L., Smithgall, T., Fujita, D.J., Ethier, S.P., and Jove, R. (1997). Constitutive activation of Stat3 in fibroblasts transformed by diverse oncoproteins and in breast carcinoma cells. *Cell Growth and Differentiation*. **8(12):** 1267-1276.

Grabner, B., Schramek, D., Mueller, K.M., Moll, H.P., Svinka, J., Hoffmann, T., Bauer, E., Blaas, L., Hruschka, N., Zboray, K., Stiedl, P., Nivarthi, H., Bogner, E., Gruber, W., Mohr, T., Zwick, R.H., Kenner, L., Poli, V., Aberger, F., Stoiber, D., Egger, G., Esterbauer, H., Zuber, J., Moriggl, R., Eferl, R., Györffy, B., Penninger, J.M., Popper, H., and Casanova, E. (2015). Disruption of STAT3 signaling promotes KRAS-induced lung tumorigenesis. *Nature Communications*. **6:6285.**

Han, Y., Amin, H.M., Franko, B., Frantz, C., Shi, X., and Lai, R. (2006). Loss of SHP1 enhances JAK3/STAT3 signaling and decreases proteasome degradation of JAK3 and NPM-ALK in ALK+ anaplastic large-cell lymphoma. *Blood*. **108(8):** 2796-2803.

He, B., You, L., Uematsu, K., Zang, K., Xu, Z., Lee, A.Y., Costello, J.F., McCormick, F., and Jablons, D.M. (2003). SOCS-3 is frequently silenced by hypermethylation and suppresses cell growth in human lung cancer. *Proc. Natl. Acad. Sci.* **100:** 14133-14138.

Hirano, T., Ishihara, K., and Hibi, M. (2000). Roles of STAT3 in mediating the cell growth, differentiation, and survival signals relayed through the IL-6 family of cytokine receptors. *Nature (Oncogene)*. **19(21):** 2548-2556.

Horvath, C.M., Wen, Z., and Darnell Jr., J.E. (1995). A STAT protein domain that determines DNA sequence recognition suggests a novel DNA-binding domain. *Genes and Development*. **9:** 984-994.

Ilaria Jr., R.L. and Van Etten, R.A. (1996). P210 and P190 (BCR/ABL) induce the tyrosine phosphorylation and DNA binding activity of multiple specific STAT family members. *J Biol Chem*. **271(49):** 31704-31710.

Irie-Sasaki, J., Sasaki, T., Matsumoto, W., Opavsky, A., Cheng, M., Welstead, G., Griffiths, E., Krawczyk, C., Richardson C.D., Aitken, K., Iscove, N., Koretzky, G., Johnson, P., Liu, P., Rothstein, D.M., and Penninger, J.M. (2001). CD45 is a JAK phosphatase and negatively regulates cytokine receptor signaling. *Nature*. **409(6818):** 349-354.

Ischenko, I., Liu, J., Petrenko, O., and Hayman, M. (2014). Transforming growth factor-beta signaling network regulates plasticity and lineage commitment of lung cancer cells. *Nature: NPG*. **(21)**: 1218-1228.

Ischenko, I., Petrenko, O., and Hayman, M.J. (2014). Analysis of the tumor-initiating and metastatic capacity of PDX1-positive cells from the adult pancreas. *PNAS*. **111(9)**: 3466-3471.

Ischenko, I., Zhi, J,, Moll, U.M., Nemajerova, A., and Petrenko, O. (2013). Direct reprogramming by oncogenic Ras and Myc. *Proc Natl Sci USA.* **110(10):** 3937-3942.

Kaptein, A., Paillard, V., and Saunders, M. (1996). Dominant negative Stat3 mutant inhibits interleukin-6-induced Jak-Stat signal transduction. *The Journal of Biological Chemistry*. **271**: 5961-5964.

Larner, A.C., Jonak, G., Cheng, Y.-S.E., Korant, B., Knight, E., and Darnell Jr., J.E. (1984). Transcriptional induction of two genes in human cells by β interferon. *Cell Biology*. **81:** 6733-6737.

Leaman, D.W., Leung, S., Li, X., and Stark, G.R. (1996). Regulation of STAT-dependent pathways by growth factors and cytokines. *FASEB J*. **10(14):** 1578-88.

Levine, R.L., Pardanani, A., Tefferi, A., and Gilliland, D.G. (2007). Role of JAK2 in the pathogenesis and therapy of myeloproliferative disorders. *Nat Rev Cancer*. **7(9):** 673-683.

Liang, H., Venema, V.J., Wang, X., Ju, H., Venema, R.C., and Marrero, M.B. (1999). Regulation of angiotensin II-induced phosphorylation of STAT3 in vascular smooth muscle cells. *Journal of Biological Chemistry*. **274(28):** 19846-19851.

Liu, L., McBride, K.M., and Reich, N.C. (2005). STAT3 nuclear import is independent of tyrosine phosphorylation and mediated by importin-α□□□*PNAS*. **102(23):** 8150-8155.

Müller, M., Briscoe, J., Laxton, C., Guschin, D., Ziemiecki, A., Silvennoinen, O., Harpur, A.G., Barbieri, G., Witthuhn, B.A., Schindler, C., *et al*. (1993). The protein tyrosine kinase JAK1 complements defects in interferon-alpha/beta and –gamma signal transduction. *Nature*. **366(6451):** 129-135.

Nair, R.R., Tolentino, J.H., and Hazlehurst, L.A. (2012). Role of STAT3 in transformation and drug resistance in CML. *Front Oncol*. **2:** 30.

Oku, S., Takenaka, K., Kuriyama, T., Shide, K., Kumano, T., Kikushige, Y., Urata, S., Yamauchi, T., Iwamoto, C., Shimoda, H.K., Miyamoto, T., Nagafuji, K., Kishimoto, J., Shimoda, K., and Akashi, K. (2010). JAK2 V617F uses distinct signaling pathways to induce cell proliferation and neutrophil activation. *Br J Haematol*. **150(3):** 334-344.

Pilati, C., Amessou, M., Bihl, M., Balabaud, C., Tran Van Nhieu, J., Paradis, V., Nault, J.C., Izard, T., Bioulac-Sage, P., and Couchy, G. (2012). Somatic mutations activating STAT3 in human inflammatory hepatocellular adenomas. *HAL*. Pgs. 1-31.

Qin, H.R., Kim, H-J., Kim, J-Y., Hurt, E.M., Klarmann, G.J., Kawasaki, B.T., Serrat, M.A.D., and Farrar, W.T. (2008). Activation of Stat3 through a phosphomimetic serine727 promotes prostate tumorigenesis independent of tyrosine705 phosphorylation. *Cancer Res.* **68(19): 7736-7741**.

Reich, N.C., and Liu, L. (2006). Tracking STAT nuclear traffic. *Nat Rev Immunol*. **6(8):** 602-612.

SBI: Systems Biosciences. (2012). *pCDH cDNA cloning and expression lentivectors: user manual*. Mountain View, CA. Systems Biosciences (SBI).

Shuai, K., Schindler, C., Prezioso, V.R., and Darnell Jr., J.E. (1992). Activation of transcription by IFN-gamma: tyrosine phosphorylation of a 91-kD DNA binding protein. *Science.* **258(5089):** 1808-1812.

Shuai, K., Horvath, C.M., Tsai Huang, T., Qureshi, S.A., Cowburn, D., and Darnell Jr., J.E. (1994). Interferon activation of the transcription factor Stat91 involves dimerization through SH2-phosphotyrosyl peptide interactions. *Cell*. **76:** 821-828.

Song, L., Turkson, J., Karras, J.G., Jove, R., and Haura, E.B. (2003). Activation of Stat3 by receptor tyrosine kinases and cytokines regulates survival in human non-small cell carcinoma cells. *Oncogene*. **22(27):** 4150-4165.

Starr, R., Willson, T.A., Viney, E.M., Murray, L.J., Rayner, J.R., Jenkins, B.J., Gonda, T.J., Alexander, W.S., Metcalf, D., Nicola, N.A., and Hilton, D.J. (1997). A family of cytokine-inducible inhibitors of signaling. *Nature*. **387(6636):** 917-921.

Tai, C.I., Schulze, E.N., and Ying, Q.L. (2014). Stat3 signaling regulates embryonic stem cell fate in a dose-dependent manner. *The Company of Biologists*. Pgs. 1-8.

Takeda, K., Noguchi, K., Shi, W., Tanaka, T., Matsumoto, M., Yoshida, N., Kishimoto, T., and Akira, S. (1997). Targeted disruption of the mouse Stat3 gene leads to early embryonic lethality. *Proc Natl Acad Sci*. **94(8):** 3801-3804.

Turkson, J., Bowman, T., Garcia, R., Caldenhoven, E., De Groot, R.P., and Jove, R. (1998). Stat3 activation by Src induces specific gene regulation and is required for cell transformation. *Mol Cell Biol.* **18(5):** 2545-2552.

Velazquez, L., Fellous, M., Stark, G.R., and Pellegrini, S. (1992). A protein tyrosine kinase in the interferon alpha/beta signaling pathway. *Cell*. **70:** 313-322.

Wegenka, U.M., Lütticken, C., Buschmann, J., Yuan, J., Lottspeich, F., Müller-Esterl, W., Schindler, C., Roeb, E., Heinrich, P.C., and Horn, F. (1994). The interleukin-6-activated acute-phase response factor is antigenically and functionally related to members of the signal transducer and activator of transcription (STAT) family. *Mol Cell Biol*. **14(5):** 3186-3196.

Wen, Z., Zhong, Z., and Darnell Jr., J.E. (1995). Maximal activation of transcription by Stat1 and Stat3 requires both tyrosine and serine phosphorylation. *Cell*. **82(2)**: 241-250.

Yang, J., Liao, X., Agarwal, M.K., Barnes, L., Auron, P.E., and Stark, G.R. (2007). Unphosphorylated STAT3 accumulates in response to IL-6 and activates transcription by binding to NFκB. *Genes and Development*. **21:** 1396-1408.

Yasukawa, H., Misawa, H., Sakamoto, H., Masuhara, M., Sasaki, A., Wakioka, T., Ohtsuka, S., Imaizumi, T., Matsuda, T., Ihle, J.N., and Yoshimura, A. (1999). The JAK-binding protein JAB inhibits Janus tyrosine kinase activity through binding in the activation loop. *EMBO J*. **18(5):** 1309-1320.

Yoshikawa, H., Matsubara, K., Qian, G.S., Jackson, P., Groopman, J.D., Manning, J.E., Harris, C.C., and Herman, J.G. (2001). SOCS-1, a negative regulator of the JAK/STAT pathway, is silenced by methylation in human hepatocellular carcinoma and shows growth-suppresive activity. *Nat Genet*. **28:** 29-35.

Yu, C.L., Meyer, D.J., Campbell, G.S., Larner, A.C., Carter-Su, C., Schwartz, J., and Jove, R. (1995). Enhanced DNA-binding activity of a Stat3-related protein in cells transformed by the Src oncoprotein. *Science*. **269(5220):** 81-83.

Zeng, G., Germinaro, M., Micsenyi, A., Monga, N.K., Bell, A., Sood, A., Malhotra, V., Sood, N., Midda, V., Monga, D.K., Kokkinakis, D.M., and Monga, S.P.S. (2006). Aberrant Wnt/β-catenin signaling in pancreatic adenocarcinoma. *Neoplasia*. **8(4):** 279-289.

Zhang, J.G., Farley, A., Nicholson, S.E., Willson, T.A., Zugaro, L.M., Simpson, R.J., Moritz, R.L., Cary, D., Richardson, R., Hausmann, G., Kile, B.T., Kent, S.B., Alexander, W.S., Metcalf, D., Hilton, D.J., Nicola, N.A., and Baca, M. (1999). The conserved SOCS box motif in suppressors of cytokine signaling binds to elongins B and C and may couple bound proteins to proteasomal degradation. *Proc Natl Acad Sci USA*. **96(5):** 2071-2076.

Zhong, Z., Wen, Z., and Darnell Jr., J.E. (1994). Stat3: a STAT family member activated by tyrosine phosphorylation in response to epidermal growth factor and interleukin-6. *Science*. **264:** 95-98.